

Covariant density functional theory for excited states in nuclei

INT, Sept. 29, 2005

Peter Ring

Technische Universität München

Content

- **Covariant Density Functional Theory**

- parametrization of the Lagrangian

- **Excitations within mean field approximation**

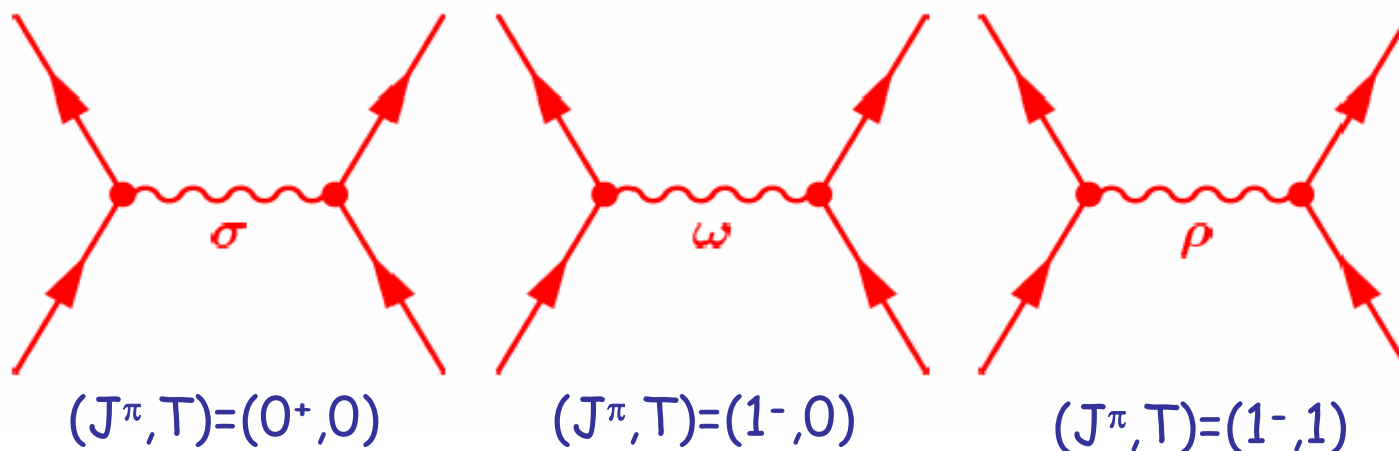
- rotational excitations (Cranked RHB)
- vibrational excitations (Rel. QRPA)

- **Methods beyond mean field**

- projected density functionals (PDFT)
- relativistic GCM
- particle vibrational coupling (PVC)
- decay width of Giant resonances

Covariant density functional theory

Nucleons are coupled by exchange of mesons through an effective Lagrangian (EFT)



$$S(\mathbf{r}) = g_\sigma \sigma(\mathbf{r})$$

↑
Sigma-meson:
attractive scalar field

$$V(\mathbf{r}) = g_\omega \omega(\mathbf{r}) + g_\rho \vec{\tau} \vec{\rho}(\mathbf{r}) + eA(\mathbf{r})$$

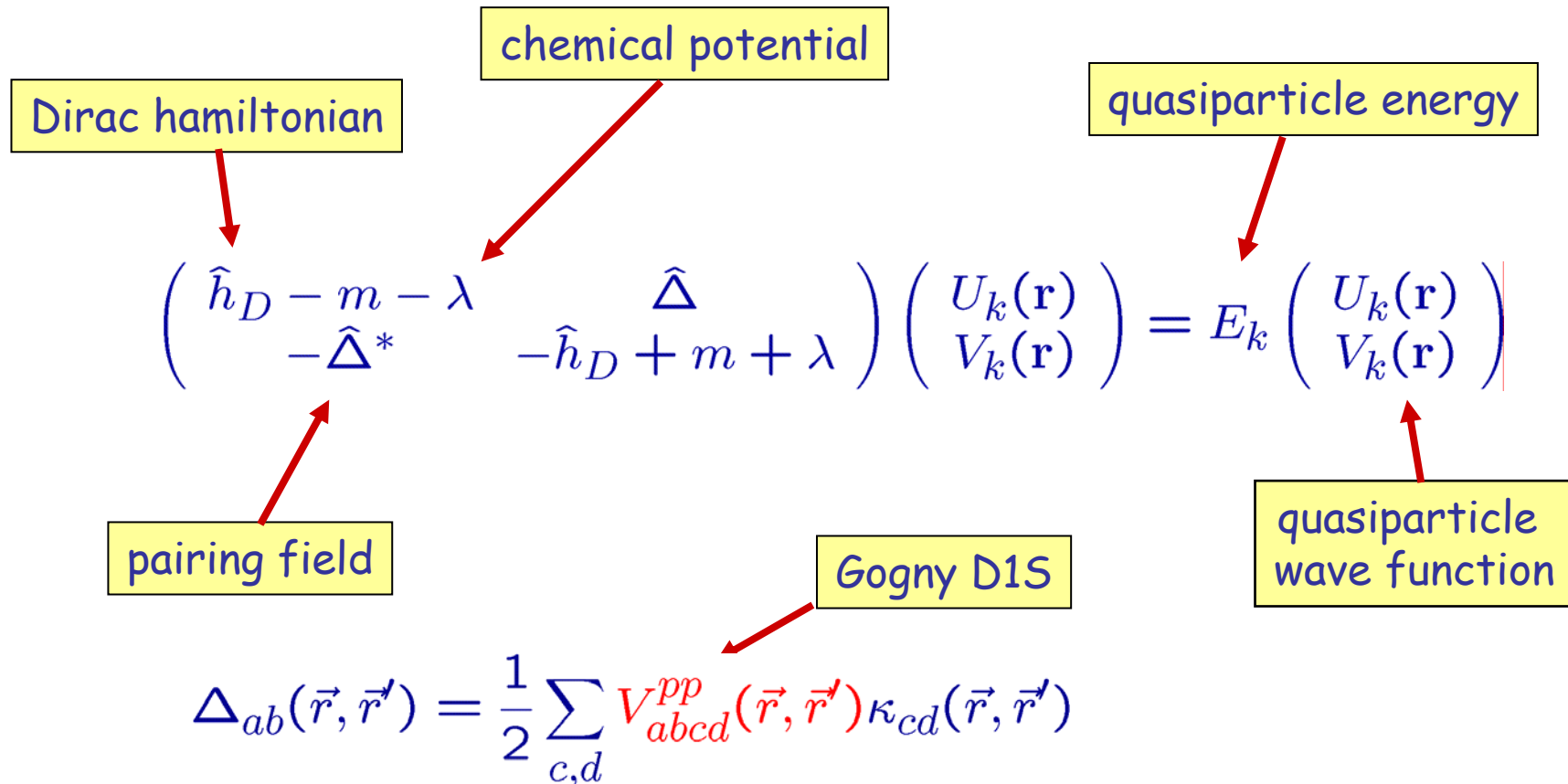
↑
Omega-meson:
short-range repulsive

↑
Rho-meson:
isovector field

Relativistic Hartree Bogoliubov (RHB)

Ground-state properties of weakly bound nuclei far from stability

→ Unified description of mean-field and pairing correlations



Effective density dependence:

non-linear potential:

NL1, NL3..

Boguta and Bodmer, NPA. 431, 3408 (1977)

$$\frac{1}{2}m_\sigma^2\sigma^2 \Rightarrow U(\sigma) = \frac{1}{2}m_\sigma^2\sigma^2 + \frac{1}{3}g_2\sigma^3 + \frac{1}{4}g_3\sigma^4$$

density dependent coupling constants:

R.Brockmann and H.Toki, PRL 68, 3408 (1992)

S.Typel and H.H.Wolter, NPA 656, 331 (1999)

$$g_o, g_\omega, g_\rho \Rightarrow g_o(\rho), g_\omega(\rho), g_\rho(\rho)$$

new

$\mathbf{g} \rightarrow \mathbf{g}(\rho(r))$

DD-ME1, DD-ME2

Niksic et al, PRC 66, 024306 (2002)
Lalazissis et al Niksic, PRC 71, 024312 (2005)

Nuclei used in the fit for DD-ME2

Nucleus	B.E (MeV)	r_c (fm)	$r_n - r_p$ (fm)	dE	dr _c	dr _{np}
¹⁶ O	127.801 (127.619)	2.727 (2.730)	-0.03	0.1	-0.1	
⁴⁰ Ca	342.741 (342.052)	3.464 (3.485)	-0.05	0.2	-0.6	
⁴⁸ Ca	414.770 (415.991)	3.481 (3.484)	0.18	-0.3	-0.1	
⁷² Ni	612.655 (613.173)	3.914	0.28	-0.1		
⁹⁰ Zr	783.155 (783.893)	4.275 (4.272)	0.07	-0.1	0.1	
¹¹⁶ Sn	986.928 (988.681)	4.615 (4.626)	0.12 (0.12)	-0.2	-0.2	3.8
¹²⁴ Sn	1048.859 (1049.962)	4.671 (4.674)	0.21 (0.19)	-0.1	-0.1	10.7
¹³² Sn	1103.469 (1102.860)	4.718	0.26	0.1		
²⁰⁴ Pb	1608.506 (1607.520)	5.500 (5.486)	0.17	0.1	0.3	
²⁰⁸ Pb	1639.826 (1636.446)	5.518 (5.505)	0.19 (0.20)	0.2	0.2	-4.7
²¹⁴ Pb	1661.182 (1663.298)	5.568 (5.562)	0.24	-0.1	0.1	
²¹⁰ Po	1649.695 (1645.228)	5.552	0.17	0.3		

Nuclear matter: $E/A=-16 \text{ MeV (5\%)}$, $\rho_0=1,53 \text{ fm}^{-3} (10\%)$
K = 250 MeV (10%), a₄ = 33 MeV (10%)

How many parameters ?

7 parameters

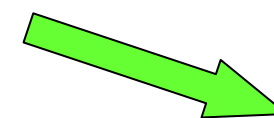
symmetric nuclear matter: $E/A, \rho_0$



$$\frac{g_\sigma}{m_\sigma}$$

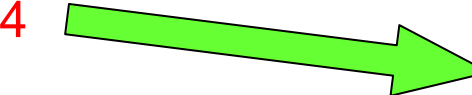
$$\frac{g_\omega}{m_\omega}$$

finite nuclei ($N=Z$): $E/A, \text{radii}$
spinorbit o.k.



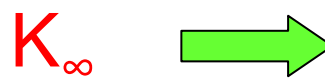
$$m_\sigma$$

($N \neq Z$): Coulomb, symmetry energy: a_4



$$\frac{g_\rho}{m_\rho}$$

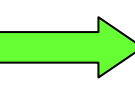
density dependence: $T=0$



$$g_2 \quad g_3$$

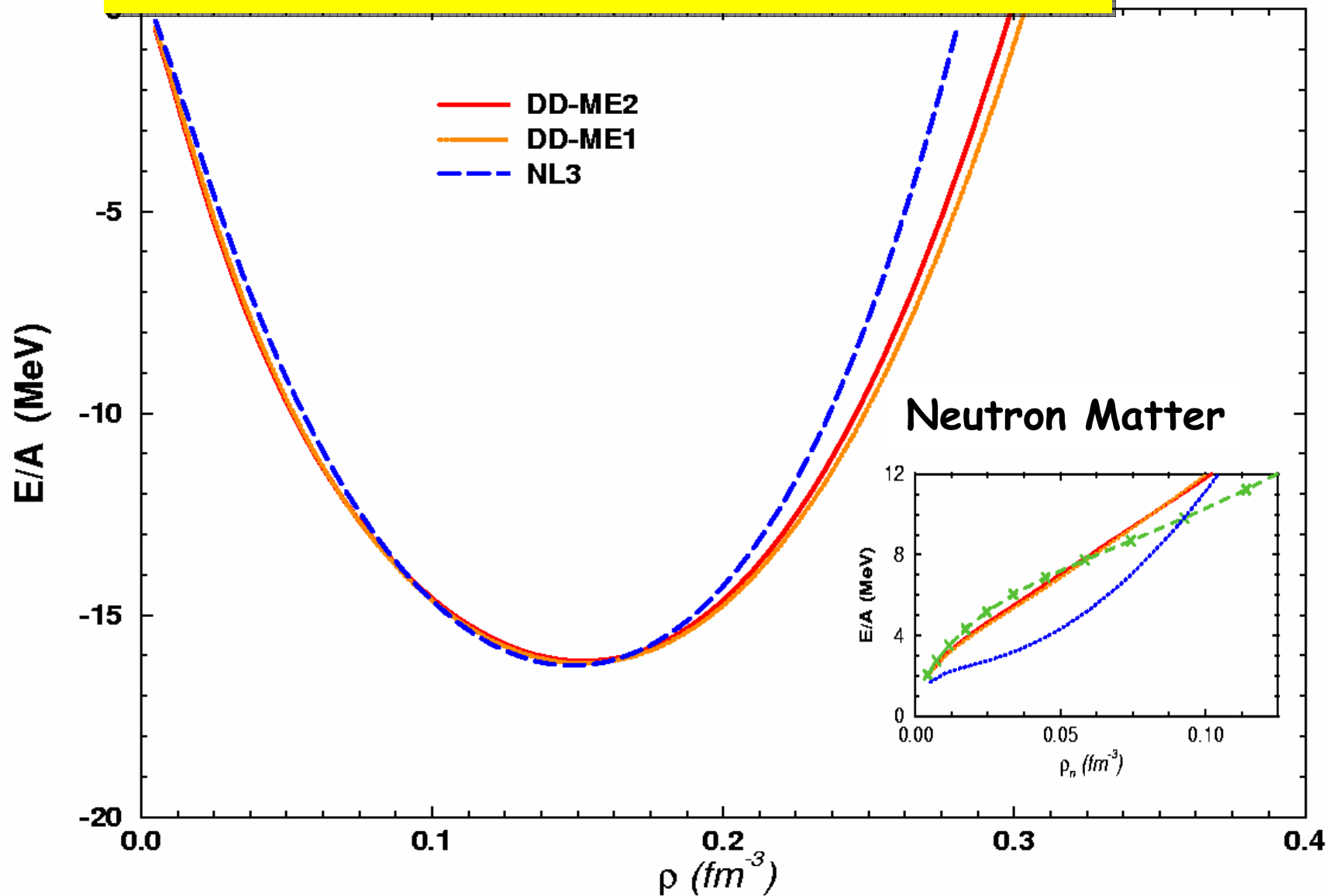
$T=1$

$$r_n - r_p$$

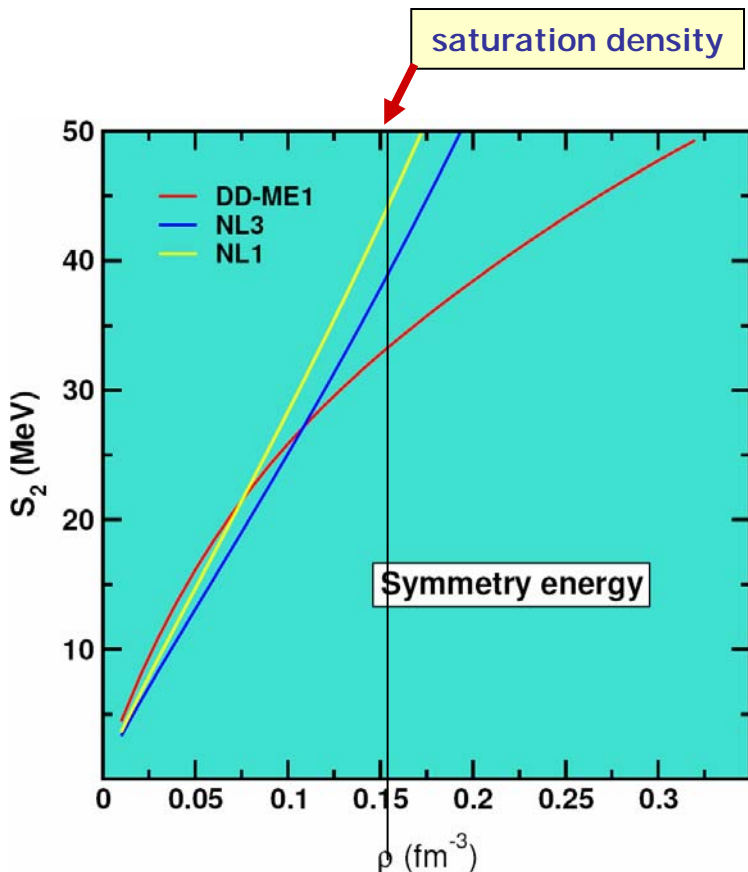


$$a_\rho$$

Nuclear matter equation of state



Symmetry energy



$$E(\rho, \alpha) = E(\rho, 0) + S_2(\rho)\alpha^2 + S_4(\rho)\alpha^4 + \dots$$

$$\alpha \equiv \frac{N-Z}{N+Z}$$

$$S_2(\rho) = a_4 + \frac{p_0}{\rho_{\text{sat}}^2} (\rho - \rho_{\text{sat}}) + \frac{\Delta K_0}{18\rho_{\text{sat}}^2} (\rho - \rho_{\text{sat}})^2 + \dots$$

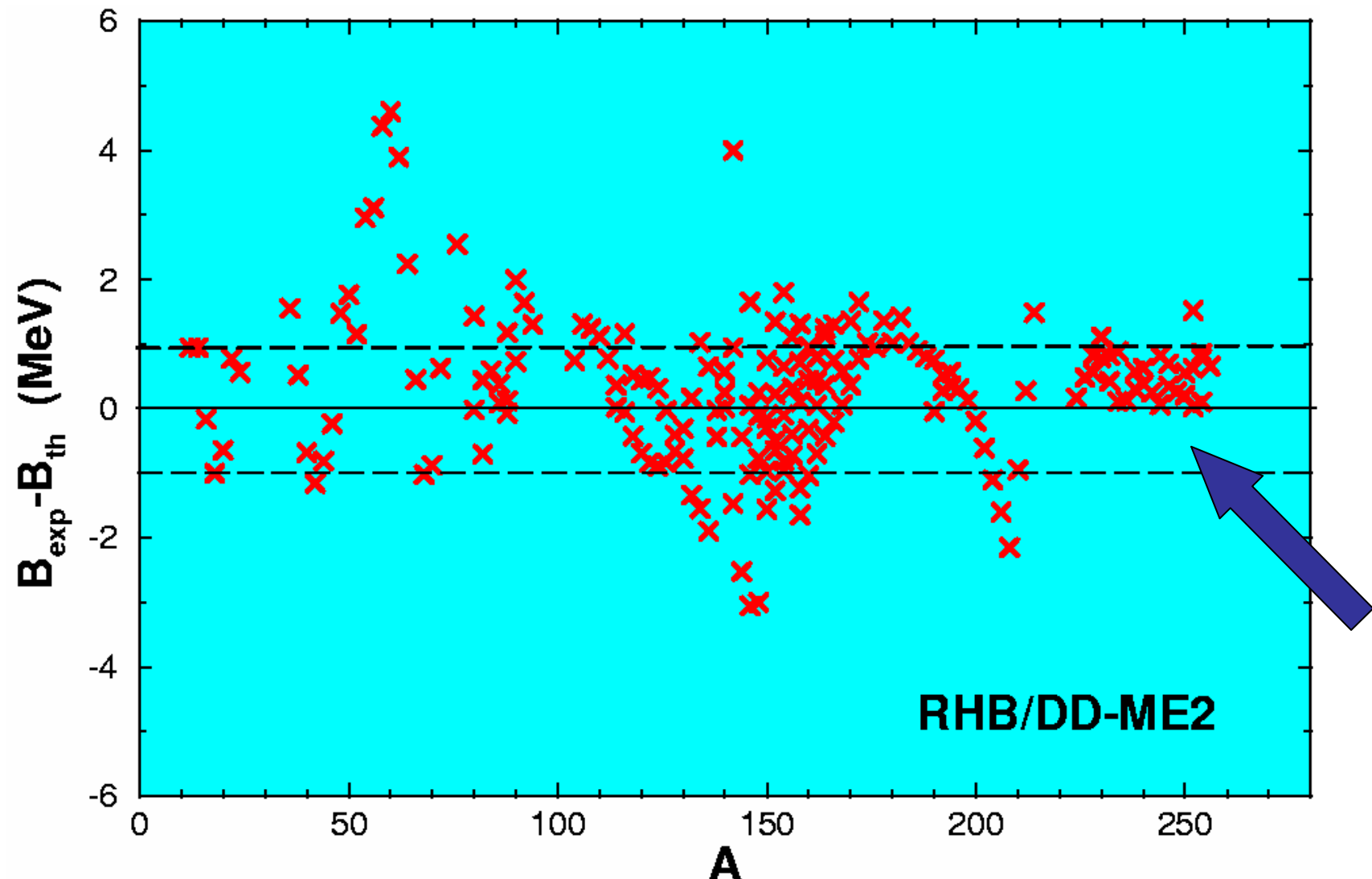
empirical values:

$$\begin{aligned} 30 \text{ MeV} < a_4 &< 34 \text{ MeV} \\ 2 \text{ MeV/fm}^3 < p_0 &< 4 \text{ MeV/fm}^3 \\ -200 \text{ MeV} < \Delta K_0 &< -50 \text{ MeV} \end{aligned}$$

	DD-ME1	NL3	NL1
$a_4(\text{MeV})$	33.1	37.9	43.7
$p_0(\text{MeV/fm}^3)$	3.26	5.92	7.0
$\Delta K_0(\text{MeV})$	-128.5	52.1	67.3

Furnstahl, NPA 705 (2002) 85

rms-deviations: masses: $\Delta m = 900 \text{ keV}$
radii: $\Delta r = 0.015 \text{ fm}$



Excited States: Time dependence:

$$\delta \int dt \left\{ \langle \Phi(t) | i\partial_t | \Phi(t) \rangle - E[\hat{\rho}(t)] \right\} = 0$$

→ $i\partial_t \hat{\rho} = [\hat{h}(\hat{\rho}) + \hat{f}, \hat{\rho}]$

Rotational Motion:

$$\rho(t) = e^{-i\vec{\Omega} t \cdot \vec{j}} \rho_\Omega e^{i\vec{\Omega} t \cdot \vec{j}}$$

$$[h - \vec{\Omega} \cdot \vec{j}, \rho_\Omega] = 0$$

Vibrational Motion:

$$\hat{\rho}(t) = \hat{\rho}^{(0)} + \delta\hat{\rho}(t)$$

$$A, B \sim \delta^2 E / \delta \rho \delta \rho$$

$$\begin{pmatrix} A & B \\ -B^* & -A^* \end{pmatrix} \begin{pmatrix} X \\ Y \end{pmatrix} = \hbar\omega \begin{pmatrix} X \\ Y \end{pmatrix}$$

↑
ground-state density

$\delta\rho_{ph}$

$\delta\rho_{hp}$

Cranked relativistic Hartree+Bogoliubov theory

CRHB equations for the fermions in the rotating frame

$$\begin{pmatrix} \hat{h}_D - \lambda_\tau - \Omega \hat{J}_x & \hat{\Delta} \\ -\hat{\Delta}^* & \hat{h}_D + \lambda_\tau + \Omega \hat{J}_x \end{pmatrix} \begin{pmatrix} U_k \\ V_k \end{pmatrix} = E_k \begin{pmatrix} U_k \\ V_k \end{pmatrix}$$

Coriolis term

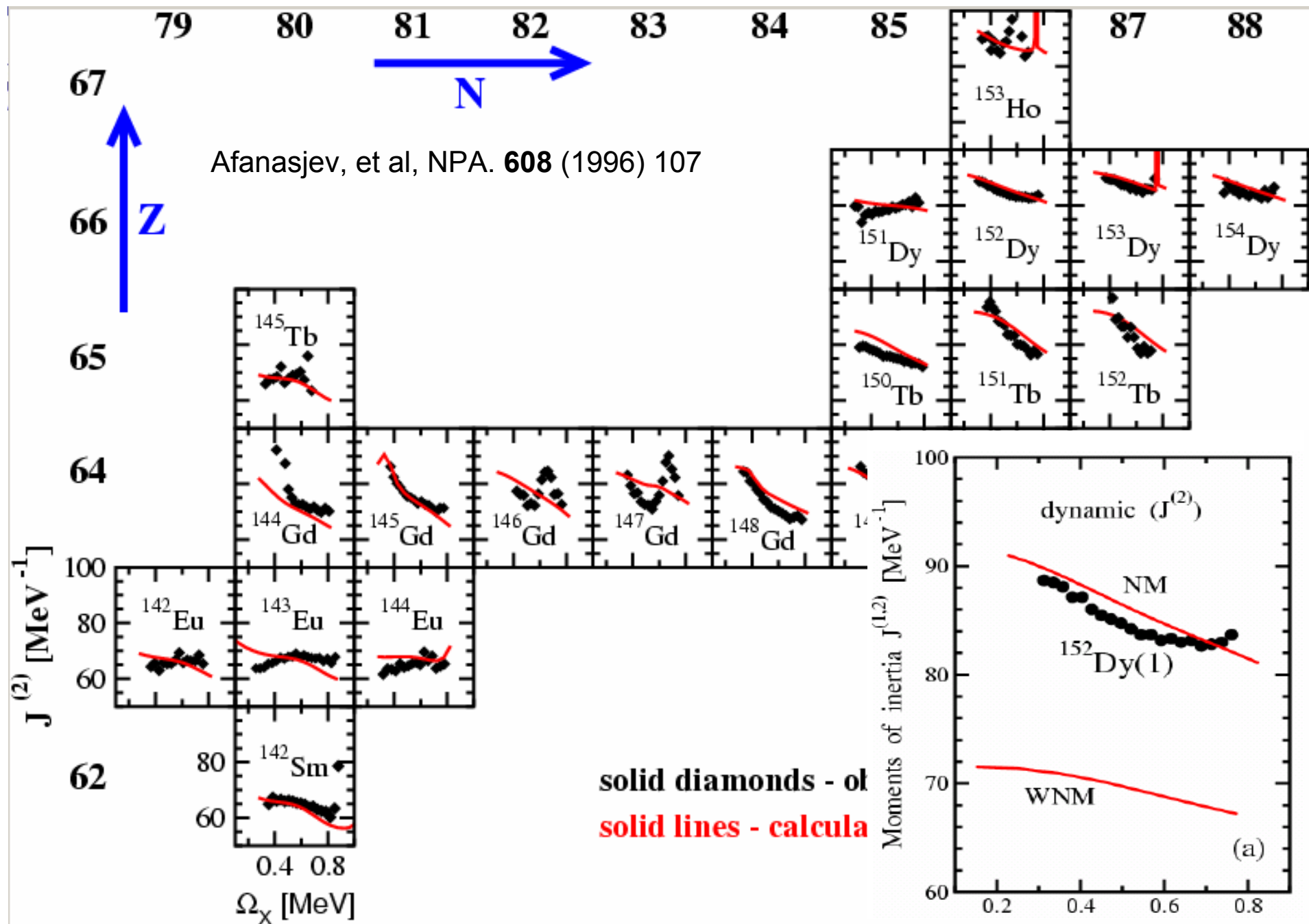
$$\hat{h}_D = \alpha(-i\vec{\nabla} - \vec{V}(\vec{r})) + V_0(\vec{r}) + \beta(m - S(\vec{r}))$$

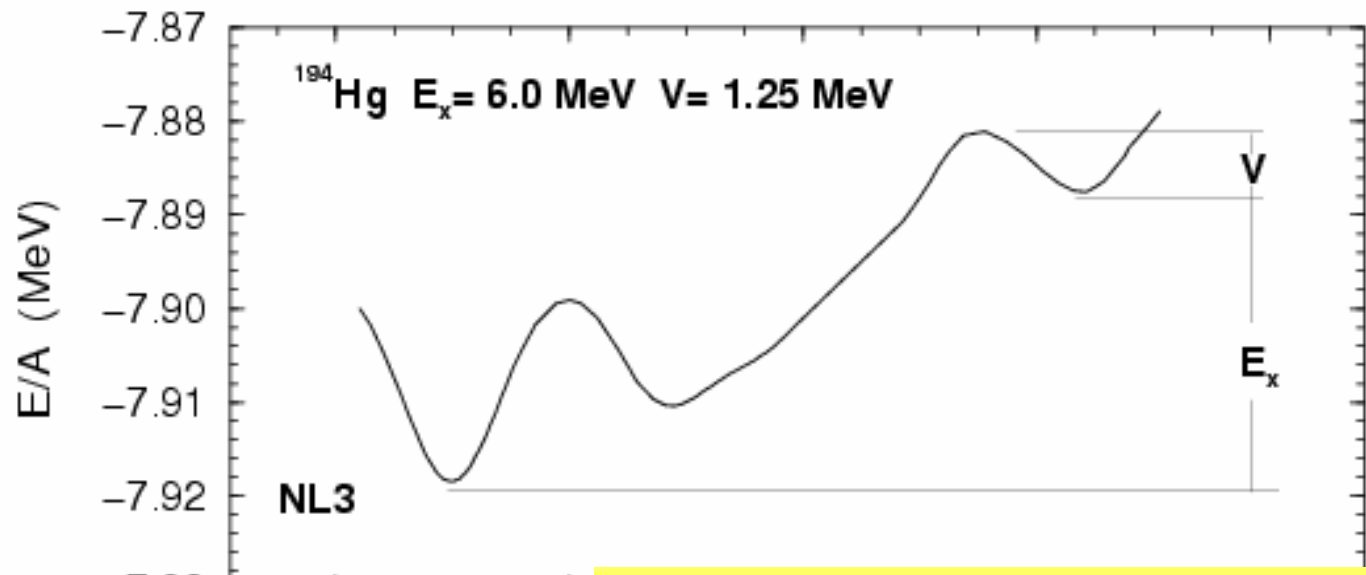
Magnetic potential

$$\vec{V}(\vec{r}) = g_\omega \vec{\omega}(\vec{r}) + g_p \tau_3 \vec{p}(\vec{r}) + e \frac{1-\tau_3}{2} \vec{A}(\vec{r})$$

space-like components of vector mesons
behaves in Dirac equation like a magnetic field

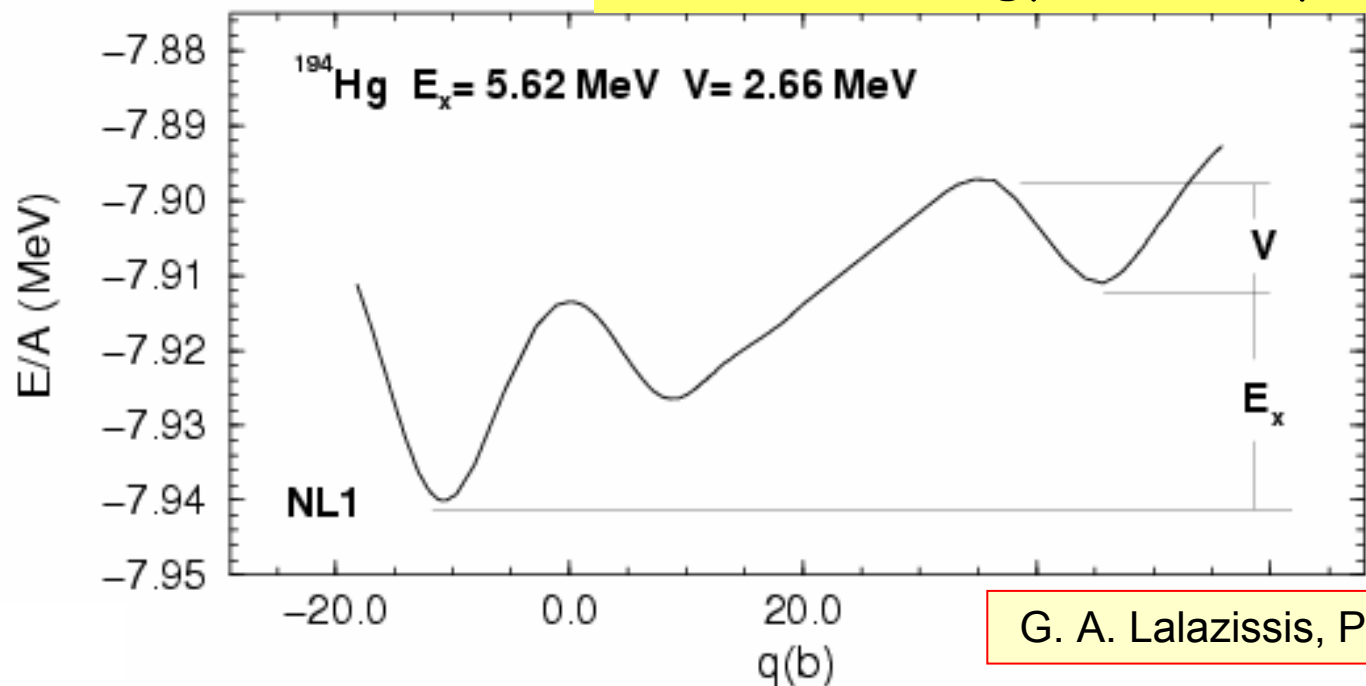
Nuclear magnetism





^{194}Hg

Excitation energy of the superdeformed minimum:

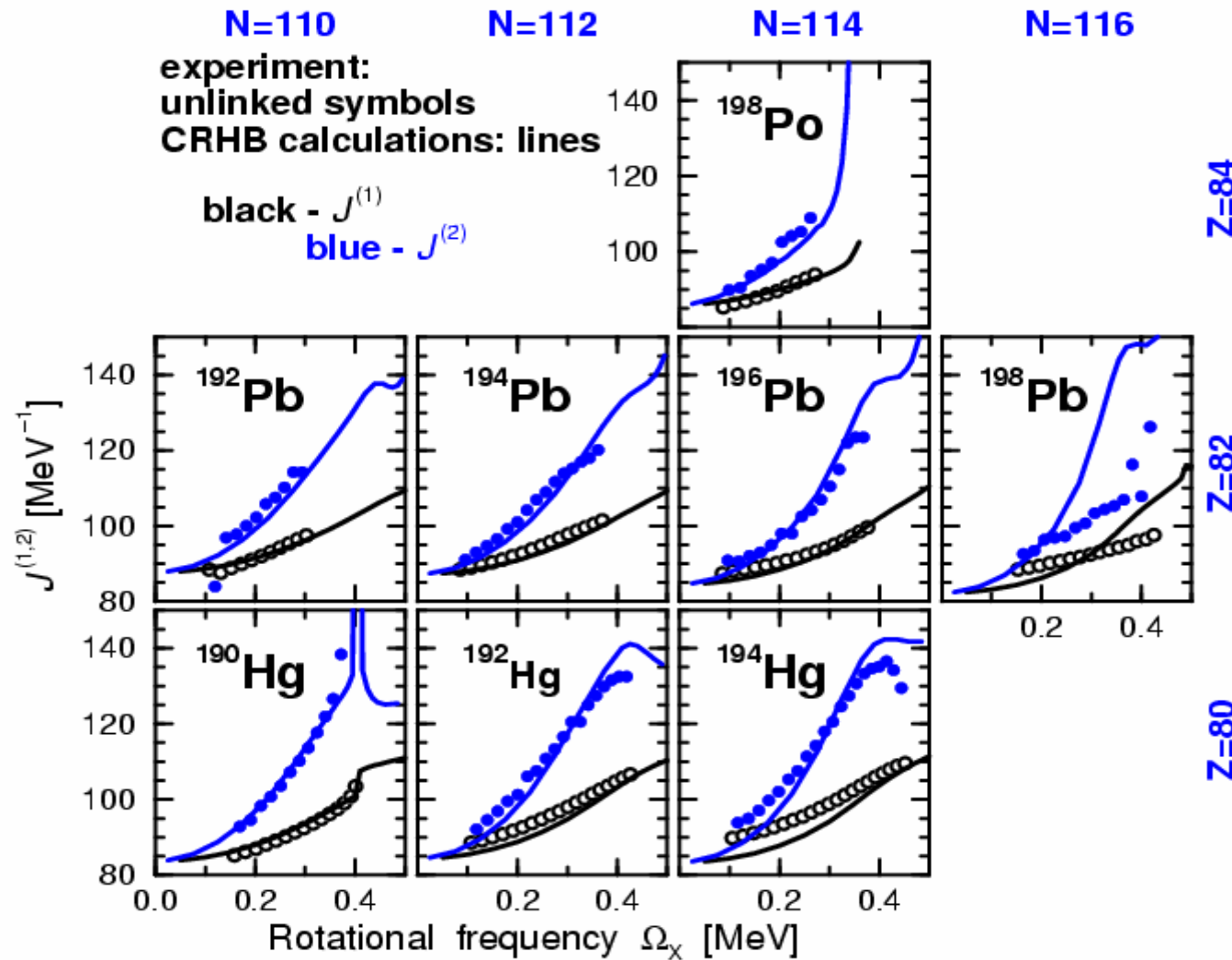


Exp:	$E_x = 6.02$
NL3:	= 6.0
NL1:	= 5.6
Gogny:	= 6.9
Skyrme:	= 5.0
WS:	= 4.6

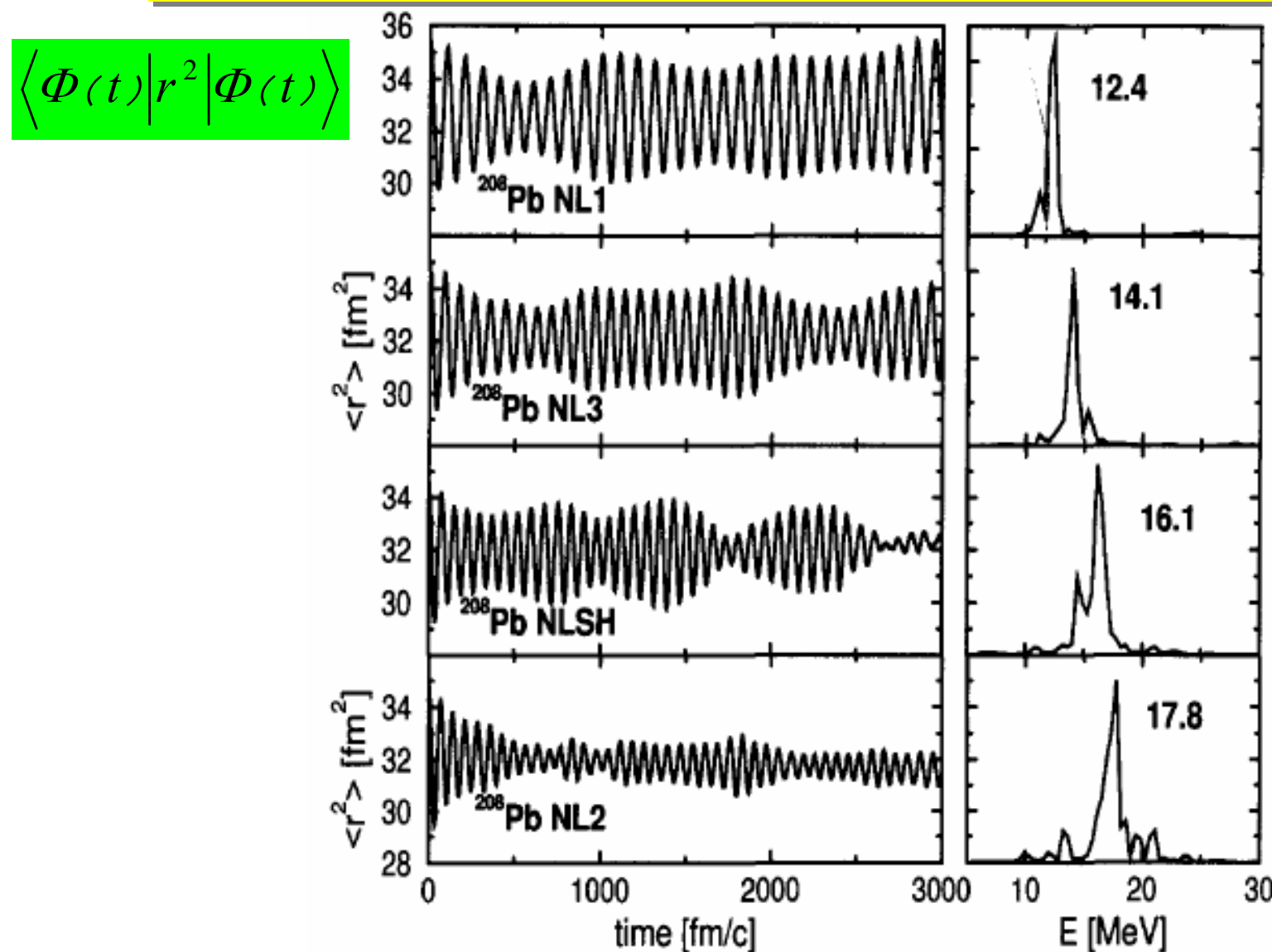
G. A. Lalazissis, P. Ring, PLB 427 (1998) 225

Cranked RHB

A.V.Afanasjev, P. Ring, J. Konig
 Phys. Rev. C60 (1999) 051303; Nucl. Phys. A 676 (2000) 196



Time-dependent RMF: breathing mode, ^{208}Pb :



$K_\infty = 211$

$K_\infty = 271$

$K_\infty = 355$

Pb: lowlying discrete spectrum

Calculated and experimental excitation energies, and $B(EL)$ values for the low-lying vibrational states in ^{208}Pb

L^π	E_{th}	E_{exp}	$B(EL)_{\text{th}}$	$B(EL)_{\text{exp}}$
3^-	2.76	2.61	499×10^3	$(540 \pm 30) \times 10^3$
5^-	3.26	3.71	201×10^6	330×10^6
2^+	4.99	4.07	2816	2965
4^+	4.95	4.32	998×10^4	1287×10^4

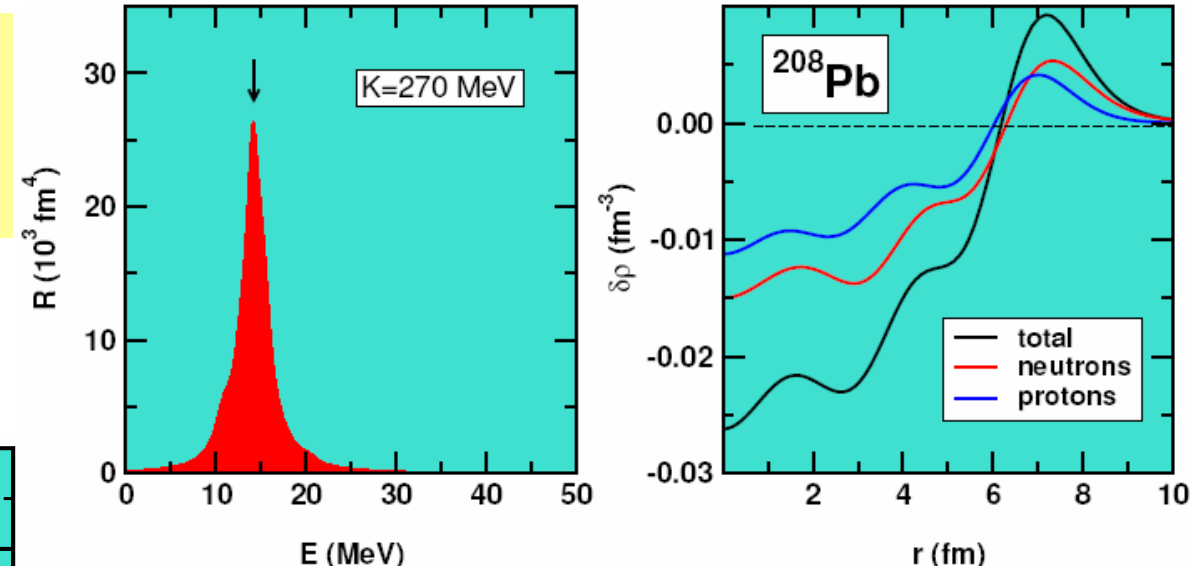
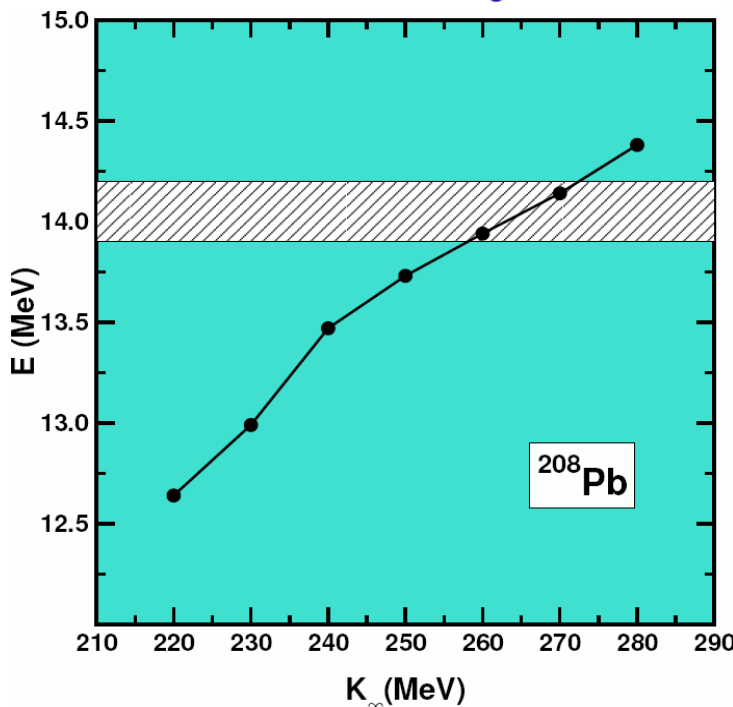
The calculated values correspond to NL3 parameterization, the data are from Ref. [29]. Energies are in MeV, $B(EL)$ values in $e^2 \text{ fm}^{2L}$.

Z.Y. Ma, A. Wandelt et al., NPA 694 (2001) 249

Isoscalar Giant Monopole Resonance: IS-GMR

The ISGMR represents the essential source of experimental information on the nuclear incompressibility

$$K_0 = p_f^2 \frac{d^2 E/A}{dp_f^2} \Big|_{p_f=0}$$



constraining the nuclear matter compressibility

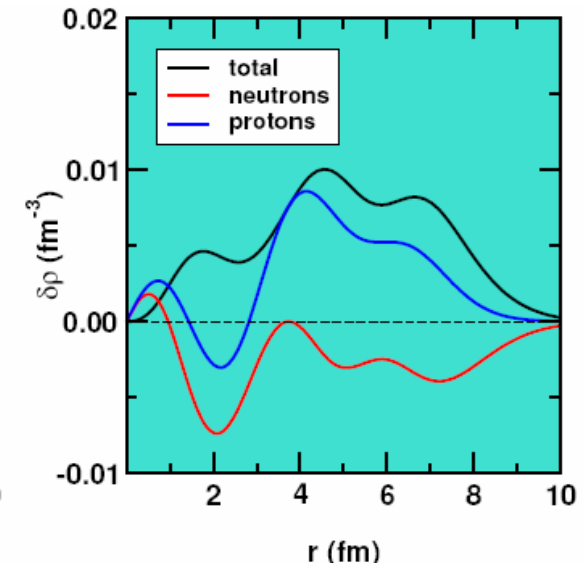
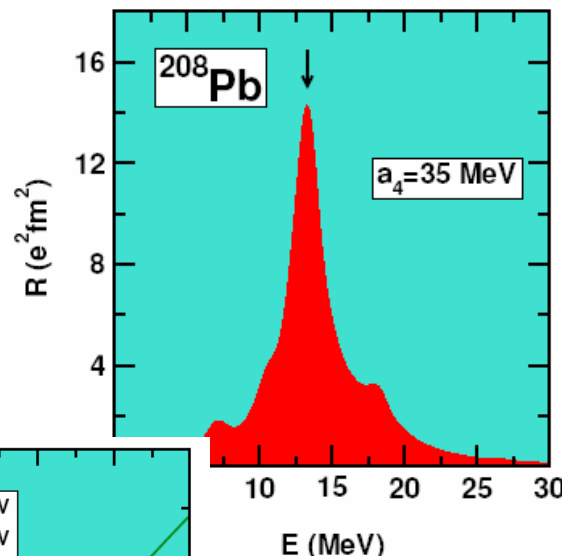
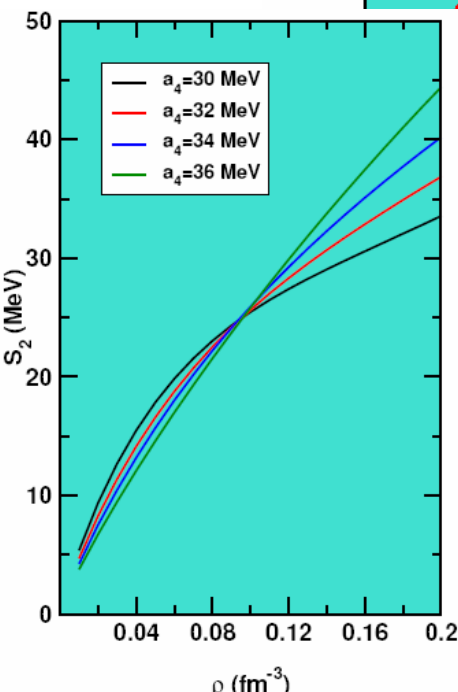
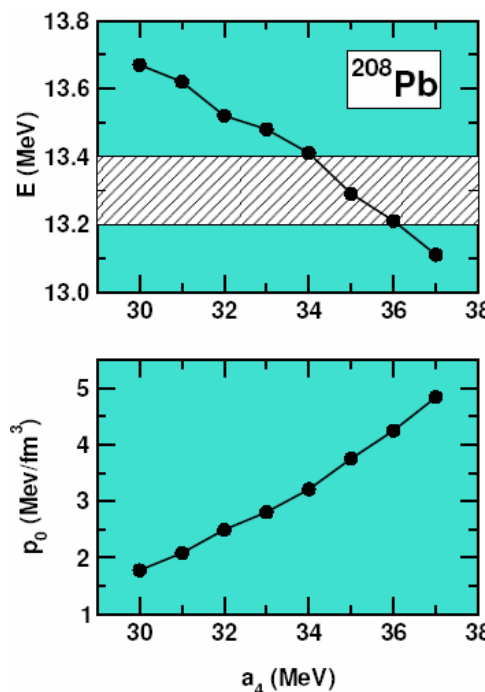


RMF models reproduce the experimental data only if

$$250 \text{ MeV} \leq K_0 \leq 270 \text{ MeV}$$

Isovector Giant Dipole Resonance: IV-GDR

the IVGDR represents one of the sources of experimental informations on the nuclear matter symmetry energy



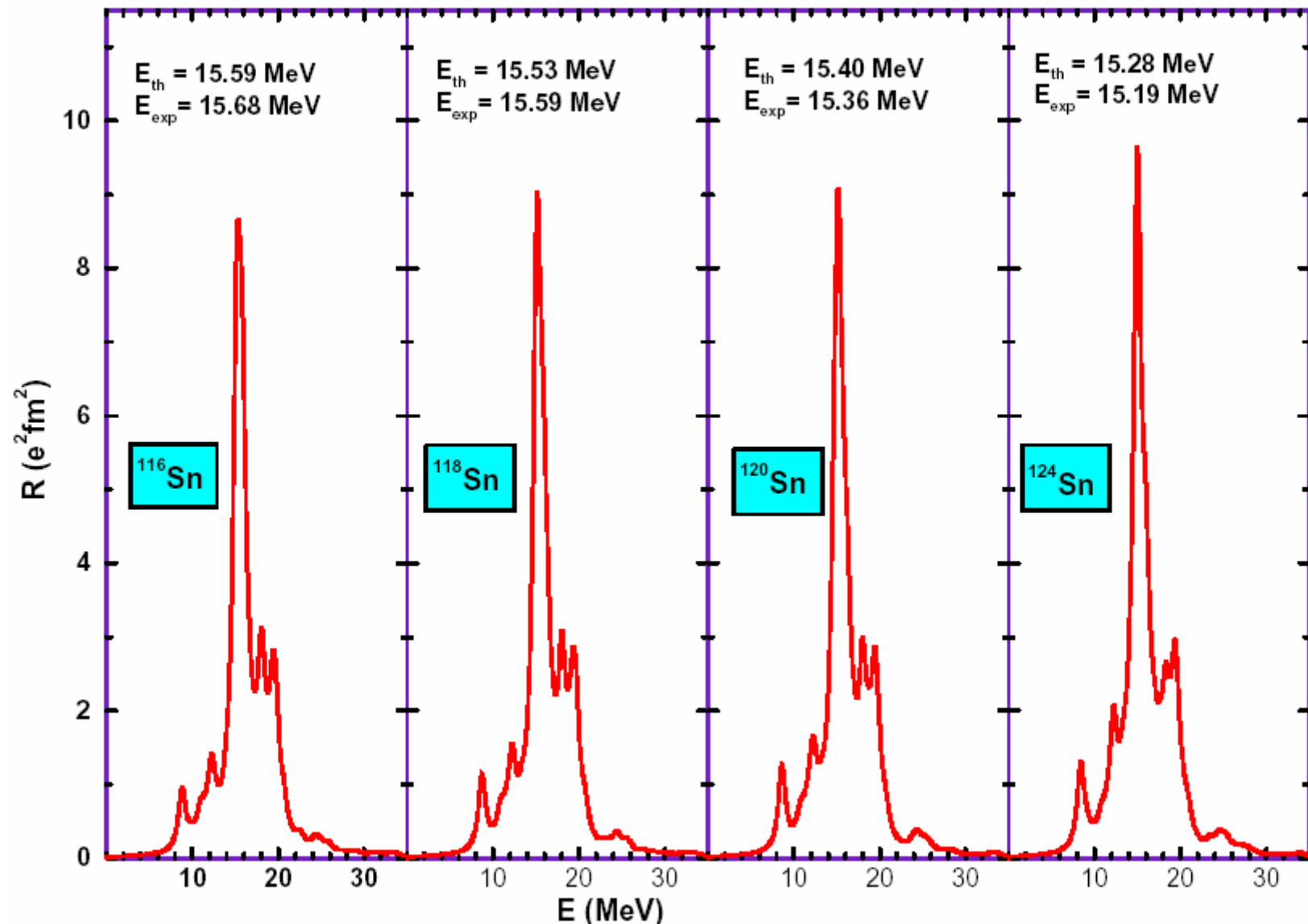
constraining the nuclear matter symmetry energy

the position of IVGDR is reproduced if

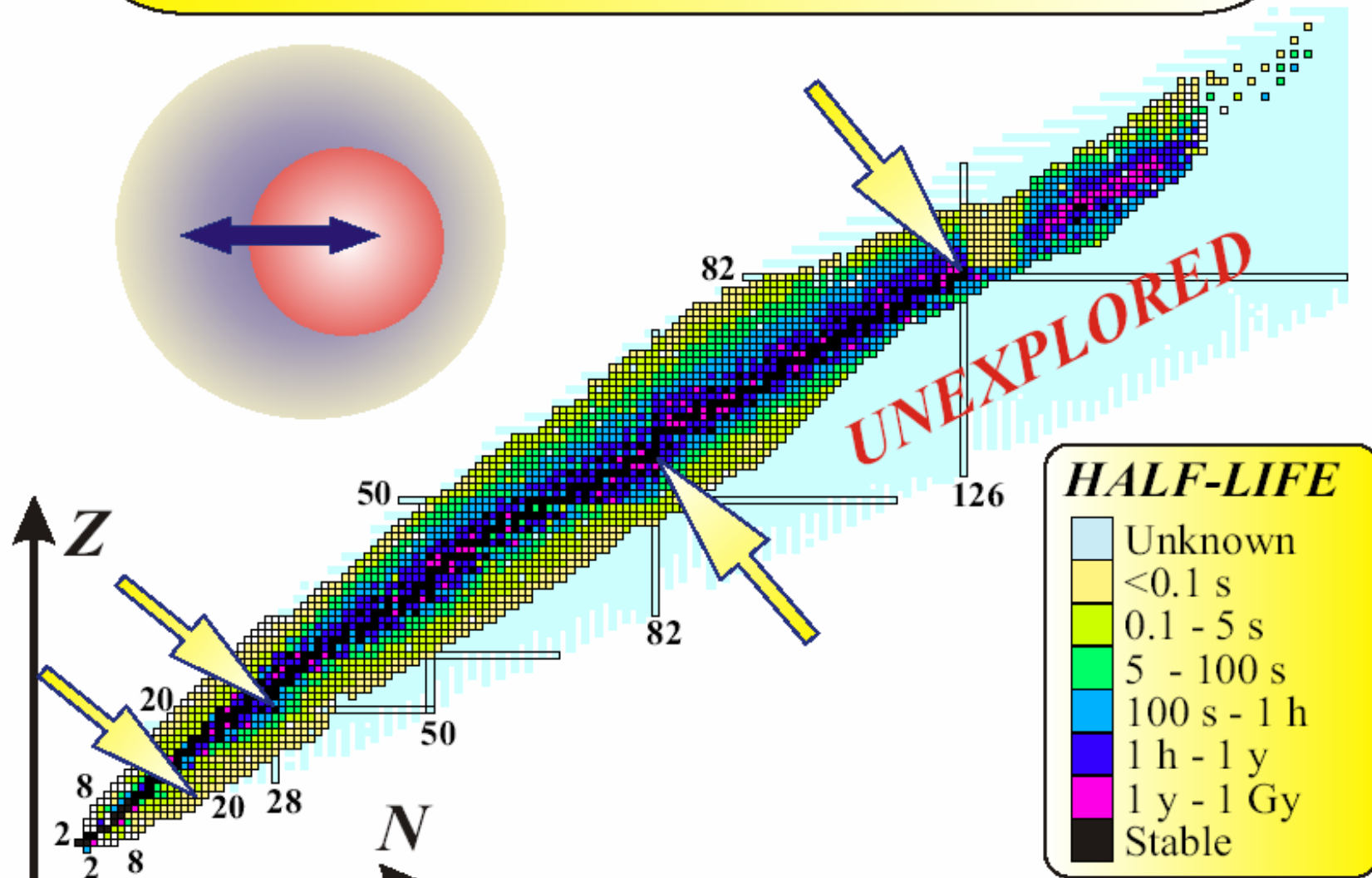
$$34 \text{ MeV} \leq a_4 \leq 36 \text{ MeV}$$

IV-GDR in Sn-isotopes

DD-ME2



Experimental indications of the soft dipole mode



Photoneutron Cross Sections for Unstable Neutron-Rich Oxygen Isotopes

A. Leistenschneider, T. Aumann, K. Boretzky, D. Cortina, J. Cub, U. Datta Pramanik, W. Dostal, Th. W. Elze, H. Emling, H. Geissel, A. Grünschloß, M. Hellstr, R. Holzmann, S. Ilievski, N. Iwasa, M. Kaspar, A. Kleinböhl, J. V. Kratz, R. Kulessa, Y. Leifels, E. Lubkiewicz, G. Münzenberg, P. Reiter, M. Rejmund, C. Scheidenberger, C. Schlegel, H. Simon, J. Stroth, K. Sümmerer, E. Wajda, W. Walus, and S. Wan

Institut für Kernphysik, Johann Wolfgang Goethe-Universität, D-60486 Frankfurt, Germany
Gesellschaft für Schwerionenforschung (GSI), D-64291 Darmstadt, Germany

Institut für Kernchemie, Johannes Gutenberg-Universität, D-55099 Mainz, Germany

Institut für Kernphysik, Technische Universität, D-64289 Darmstadt, Germany

Instytut Fizyki, Uniwersytet Jagielloński, PL-30-059 Kraków, Poland

Sektion Physik, Ludwig-Maximilians-Universität, D-85748 Garching, Germany

(Received 19 December 2000)

The dipole response of stable and unstable neutron-rich oxygen nuclei of masses $A=17$ to $A=22$ has been investigated experimentally utilizing electromagnetic excitation in heavy-ion collisions at beam energies about 600 MeV/nucleon. A kinematically complete measurement of the neutron decay channel in inelastic scattering of the secondary beam projectiles from a Pb target was performed. Differential electromagnetic excitation cross sections $d\sigma/dE$ were derived up to 30 MeV excitation energy. In contrast to stable nuclei, the deduced dipole strength distribution appears to be strongly fragmented and systematically exhibits a considerable fraction of low-lying strength.

DOI: 10.1103/PhysRevLett.86.2560

The study of the response of a clear or electromagnetic field is the properties of the nuclear reaction energies above the particle response of stable nuclei is dominant of various multipolarities, the giant resonance strength stable to exotic weakly bound neutron-to-proton ratios is presently unclear. For neutron-rich nuclei, more pronounced effects, in particular strength towards lower excitations in the giant resonance region. The probabilities depend strongly on the effective interactions. In turn, measurements response of exotic nuclei can depend on the isospin dependence of nucleon-nucleon interaction [7].

Systematic experimental information on the response of exotic nuclei, however, is limited. For some light halo nuclei, low-energy excitations have been observed in electromagnetic dissociation [8–11]. For the one-neutron halo nucleus ^{11}C [11], the observed dipole excitation energies was interpreted as a threshold effect, involving nonvalence neutron into the continuum. He and ^{7}Li , a coherent dipole neutron against the core was observed. The appearance of a collective state general was predicted for ^{11}C [19,20], located at excitation energies near the dipole resonance (GDR) [19].

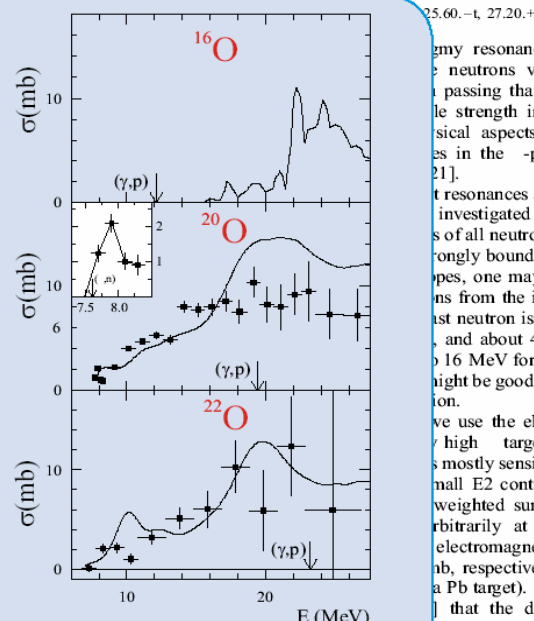


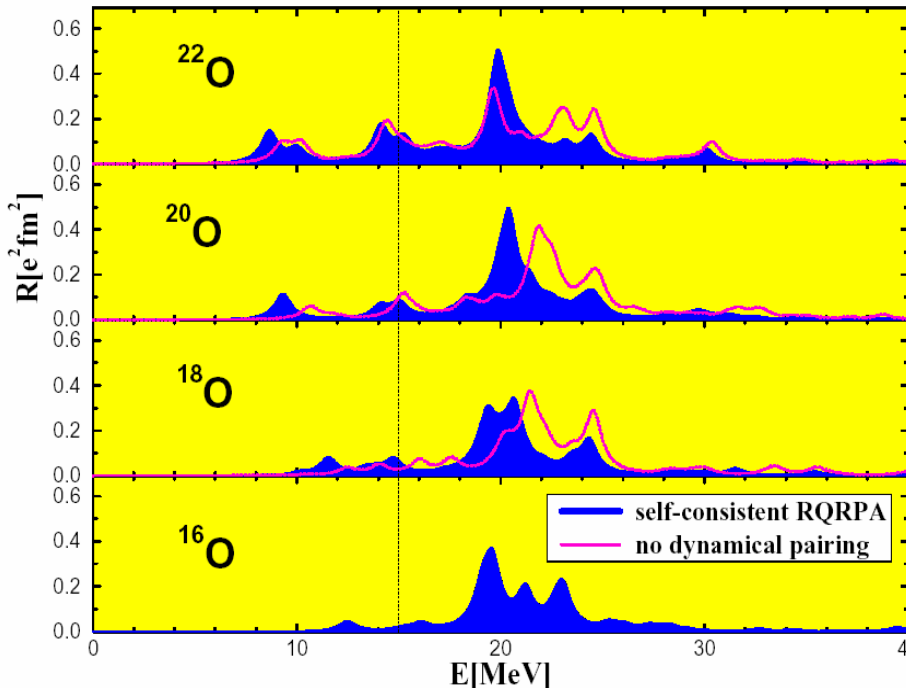
FIG. 2. Photoneutron cross sections σ for ^{16}O (upper panel) and for the unstable isotopes $^{20,22}\text{O}$ (lower panels) as extracted from the measured electromagnetic excitation cross sections (symbols). The inset displays the cross section for ^{16}O near the neutron threshold on an expanded energy scale. The thresholds for decay channels involving protons (which were not observed in the present experiment) are indicated by arrows.

gym resonance, may arise when neutrons vibrate against the passing that a systematic study of the dipole strength in neutron-rich nuclei aspects, e.g., calculations in the β -process of the ^{21}O .

Resonances and lower lying states have been investigated systematically for all neutron-rich oxygen isotopes, one may expect a dependence of the dipole strength from the inert ^{16}O core. The first neutron is 7–8 MeV for ^{17}O , and about 4 MeV for the ^{18}O and 16 MeV for ^{20}O . Thus the ^{20}O and ^{22}O might be good candidates for the β -process.

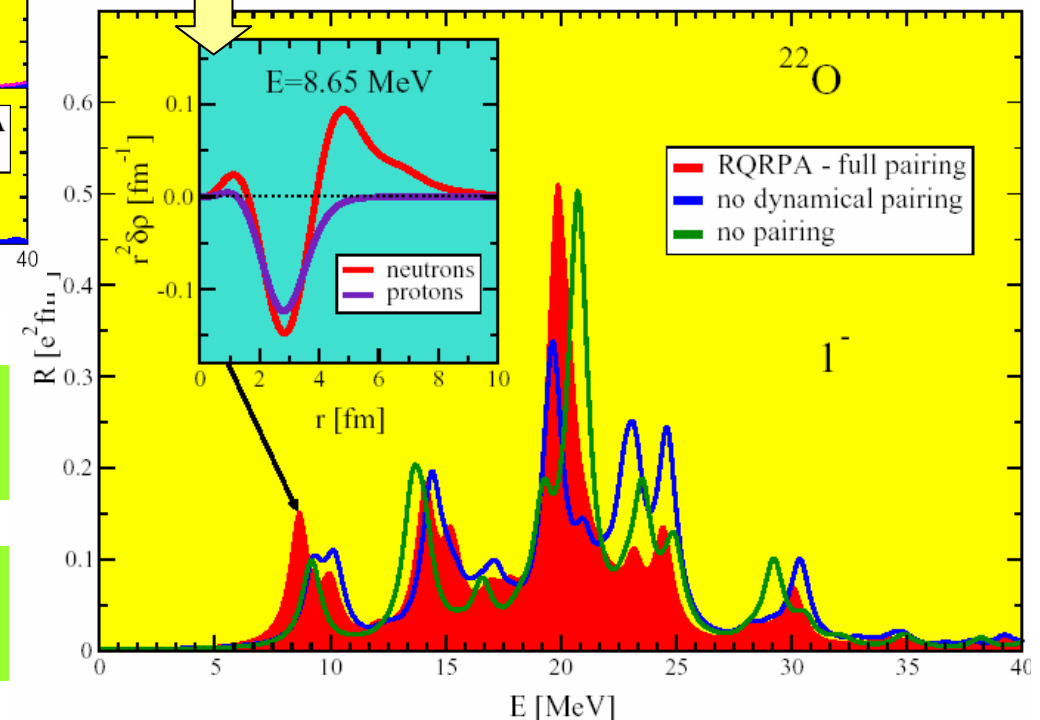
We use the electromagnetic dissociation on high energy targets. Similar to the case of ^{16}O , it is mostly sensitive to electric dipole (E1) and small E2 contributions. For the weighted sum rule for E1 and E2, arbitrarily at an excitation energy of 30 MeV, we find $\sigma_{\text{E1}} = 10 \text{ mb}$, respectively (calculated for ^{16}O on a Pb target). It was demonstrated that the dipole strength can be deduced quantitatively from a measurement of the electromagnetic dissociation cross section and the corresponding parameters by applying the method of the β -process [24]. The high secondary beam energy of 600 MeV/nucleon allows for the

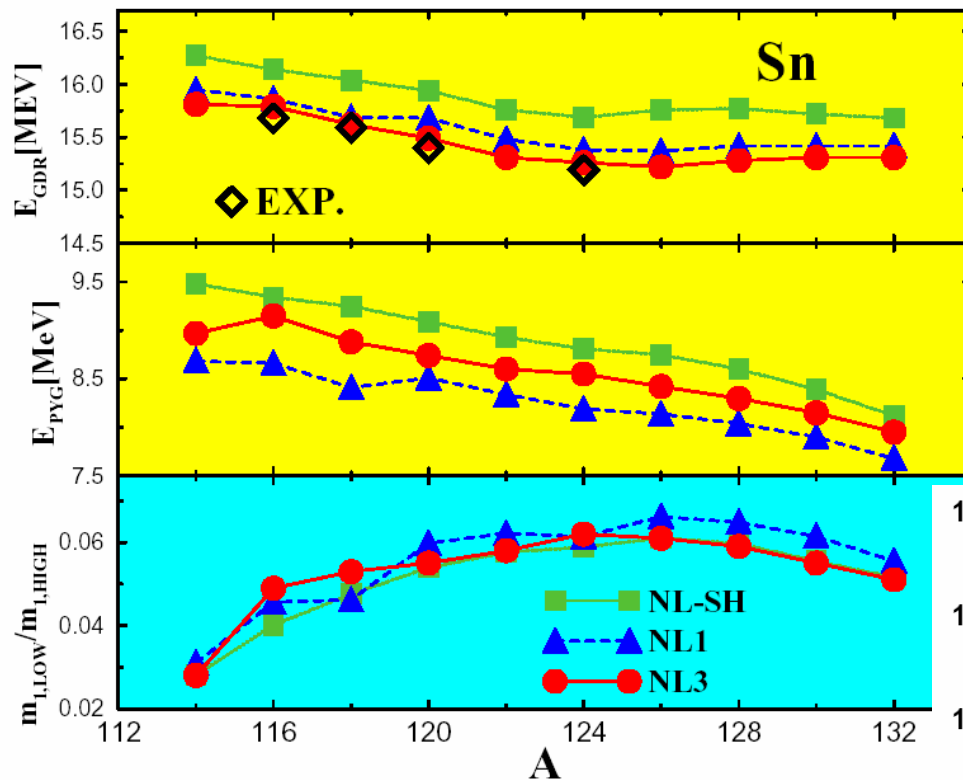
Evolution of IV dipole strength in Oxygen isotopes



RHB + RQRPA calculations with the NL3 relativistic mean-field plus D1S Gogny pairing interaction.

Transition densities





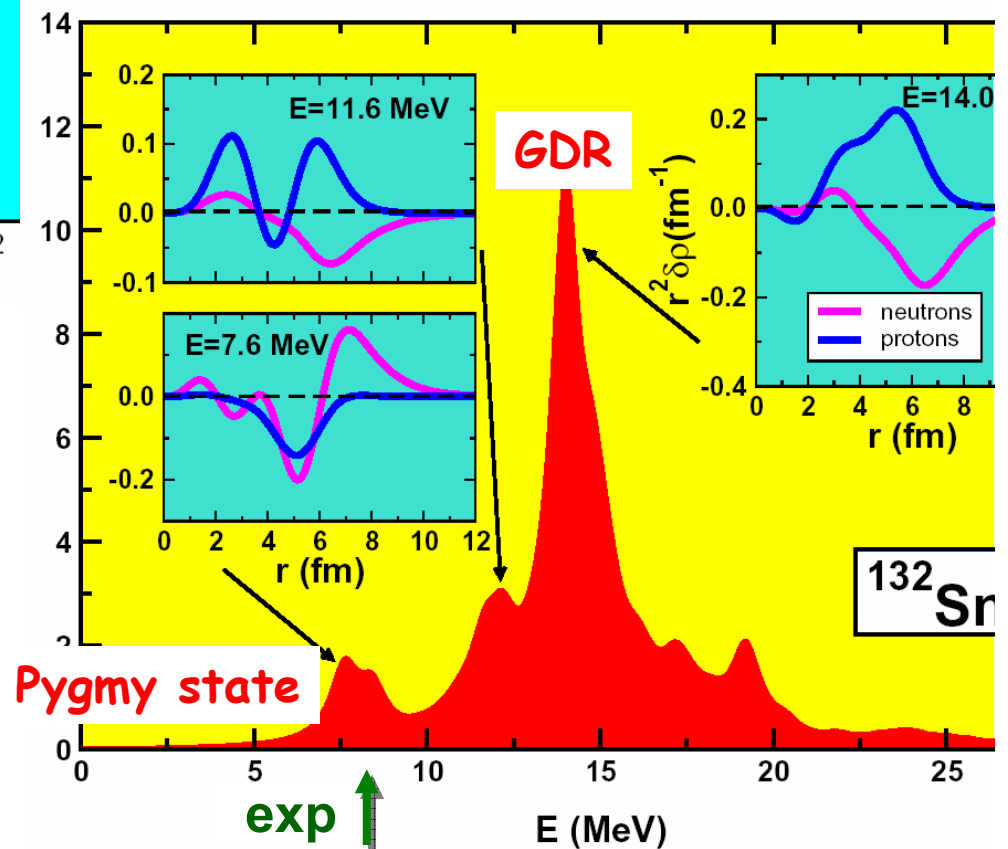
Mass dependence of GDR and Pygmy dipole states in Sn isotopes. Evolution of the low-lying strength.

Isovector dipole strength in ^{132}Sn .

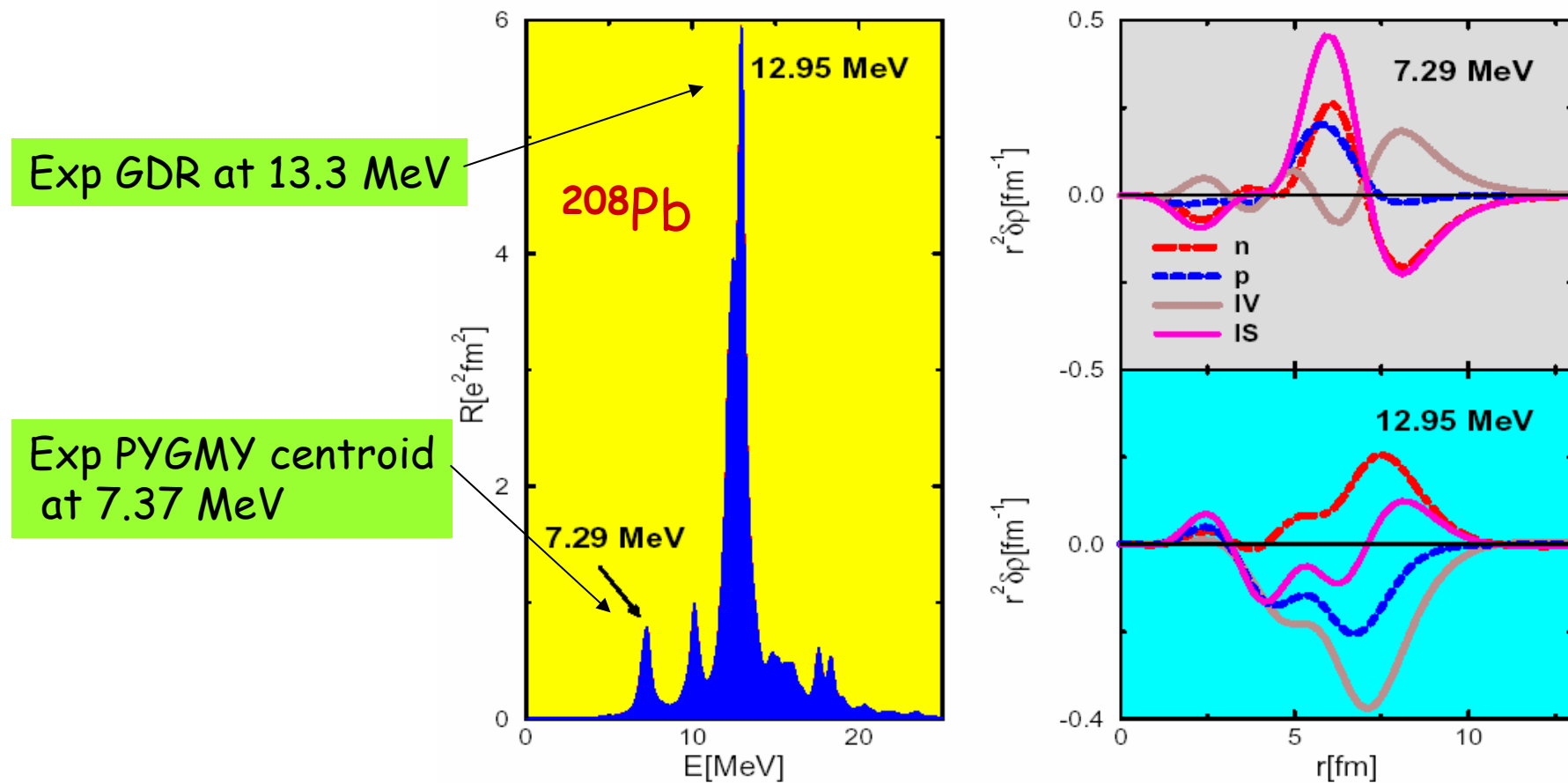
Nucl. Phys. A692, 496 (2001)

Distribution of the neutron particle-hole configurations for the peak at 7.6 MeV (1.4% of the EWSR)

^{132}Sn at 7.6 MeV	
28.2%	$2d_{3/2} \rightarrow 2f_{5/2}$
21.9%	$2d_{5/2} \rightarrow 2f_{7/2}$
19.7%	$2d_{3/2} \rightarrow 3p_{1/2}$
10.5%	$1h_{11/2} \rightarrow 1i_{13/2}$
3.5%	$2d_{5/2} \rightarrow 3p_{3/2}$
1.9%	$1g_{7/2} \rightarrow 2f_{5/2}$
1.5%	$1g_{7/2} \rightarrow 1h_{9/2}$
0.6%	$1g_{7/2} \rightarrow 2f_{7/2}$
0.6%	$2d_{3/2} \rightarrow 3p_{3/2}$

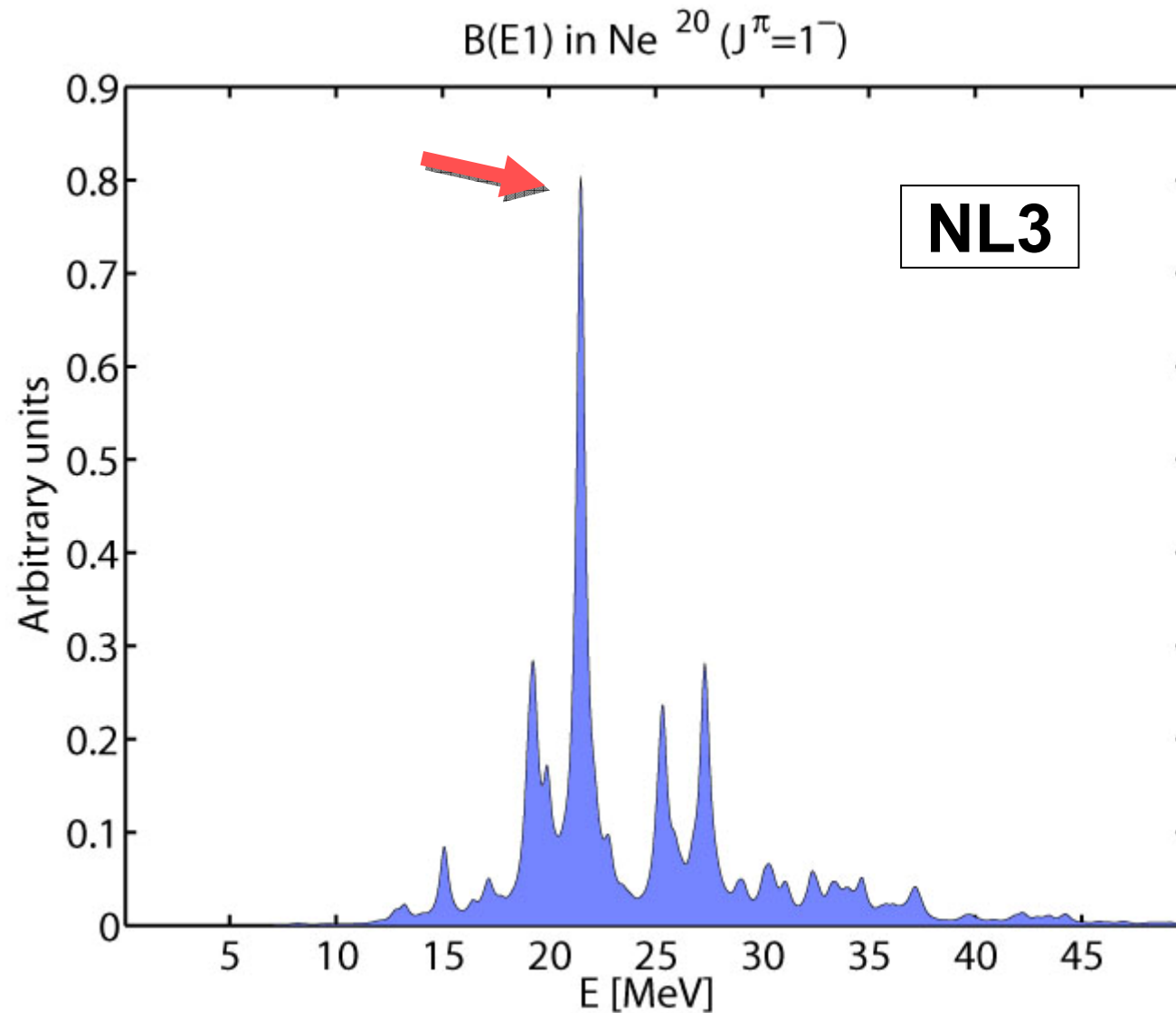


IV Dipole Strength for ^{208}Pb and transition densities
for the peaks at 7.29 MeV and 12.95 MeV PRC 63, 047301 (2001)

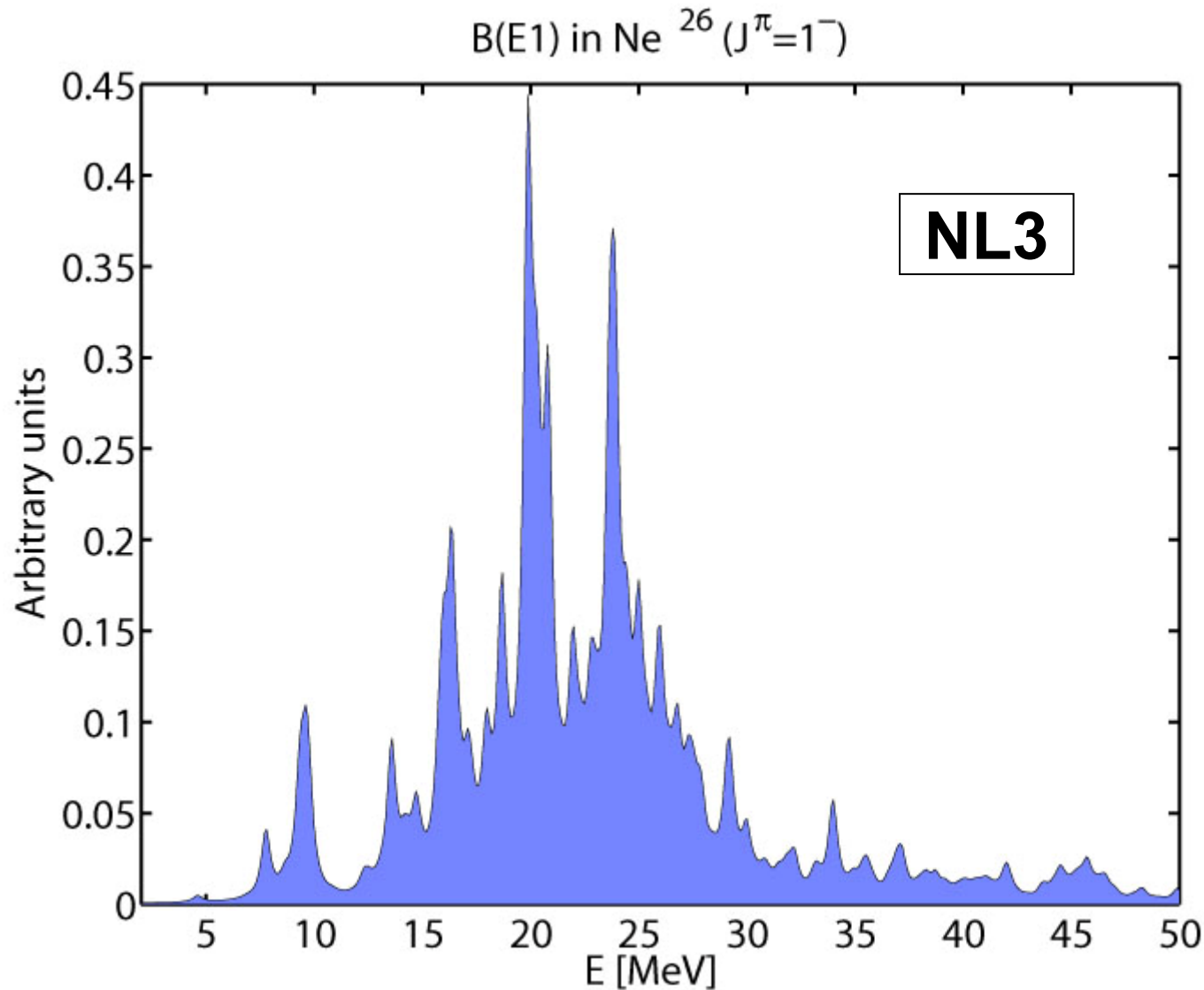


In heavier nuclei low-lying dipole states appear that are characterized by a more distributed structure of the RQRPA amplitude.

E1-strength distribution in deformed ^{20}Ne

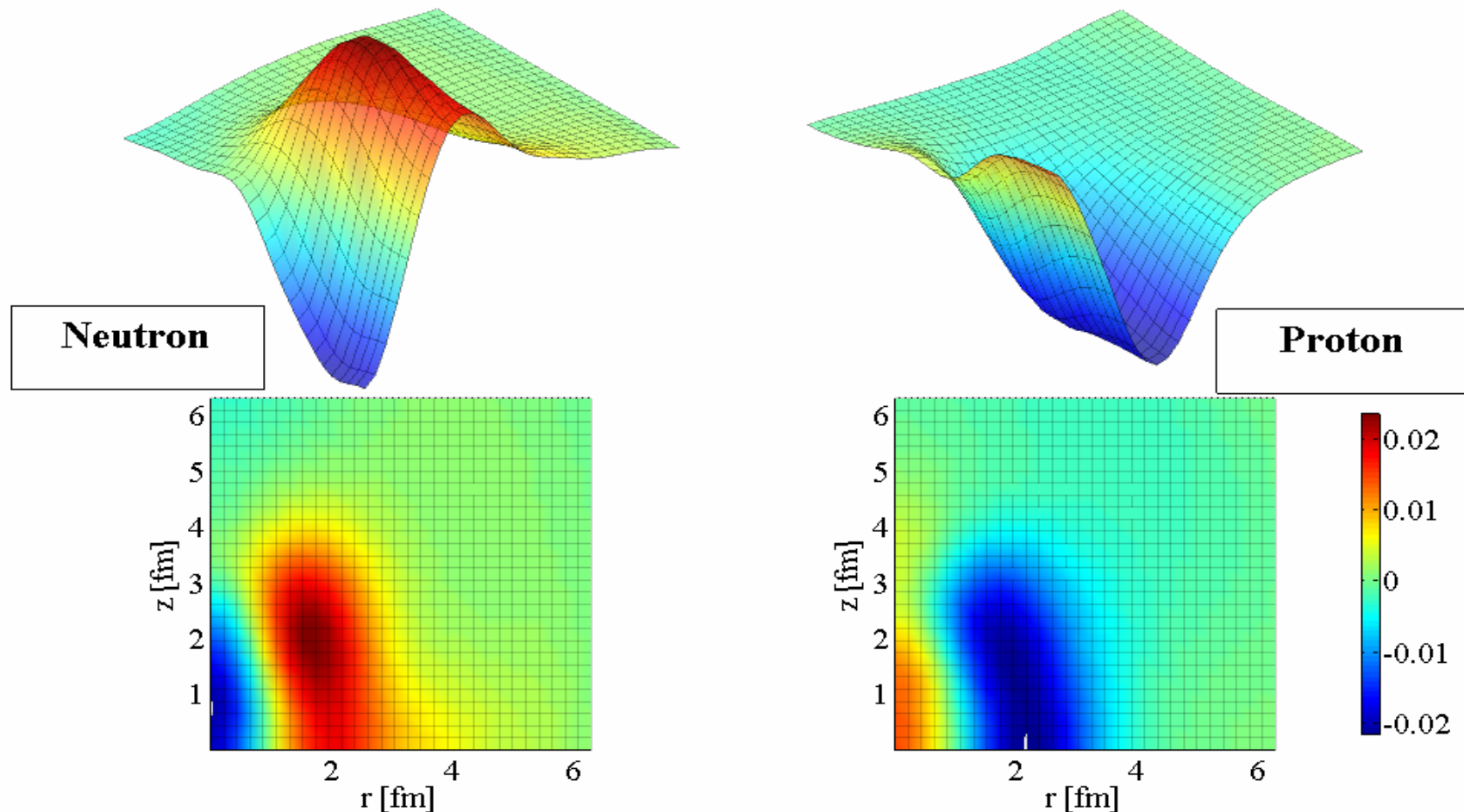


IV-E1-Resonances in deformed ^{26}Ne



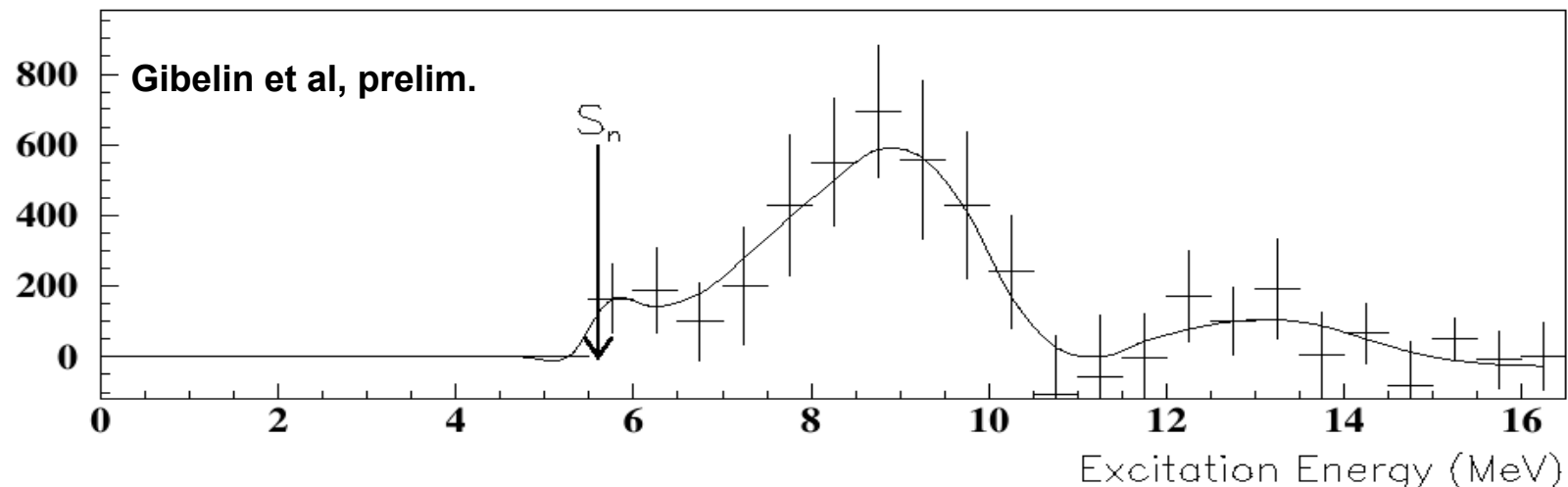
Transition density of the upper E1-peak

E1 Ne^{20} Transition Density, Peak at 21.4 MeV

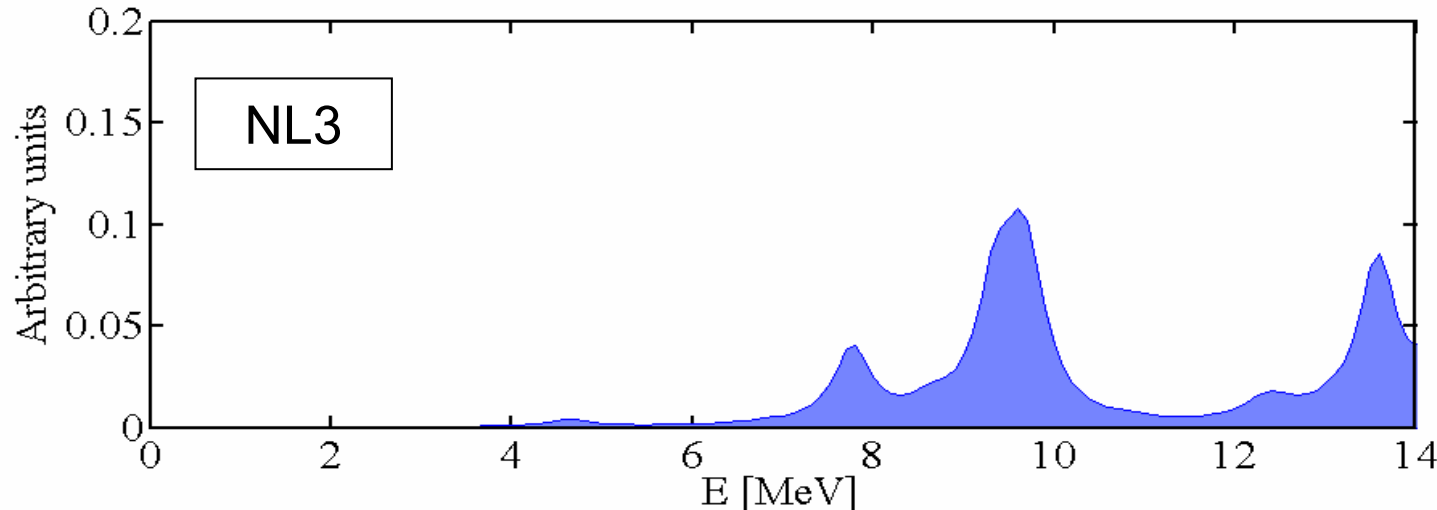


Pygmy-Resonance in deformed ^{26}Ne

Counts



Low Lying $B(E1)$ in Ne^{26} ($J^\pi=1^-$)



Isoscalar dipole compression - toroidal modes

Isoscalar GMR in spherical nuclei \rightarrow nuclear matter compression modulus K_{nm} .

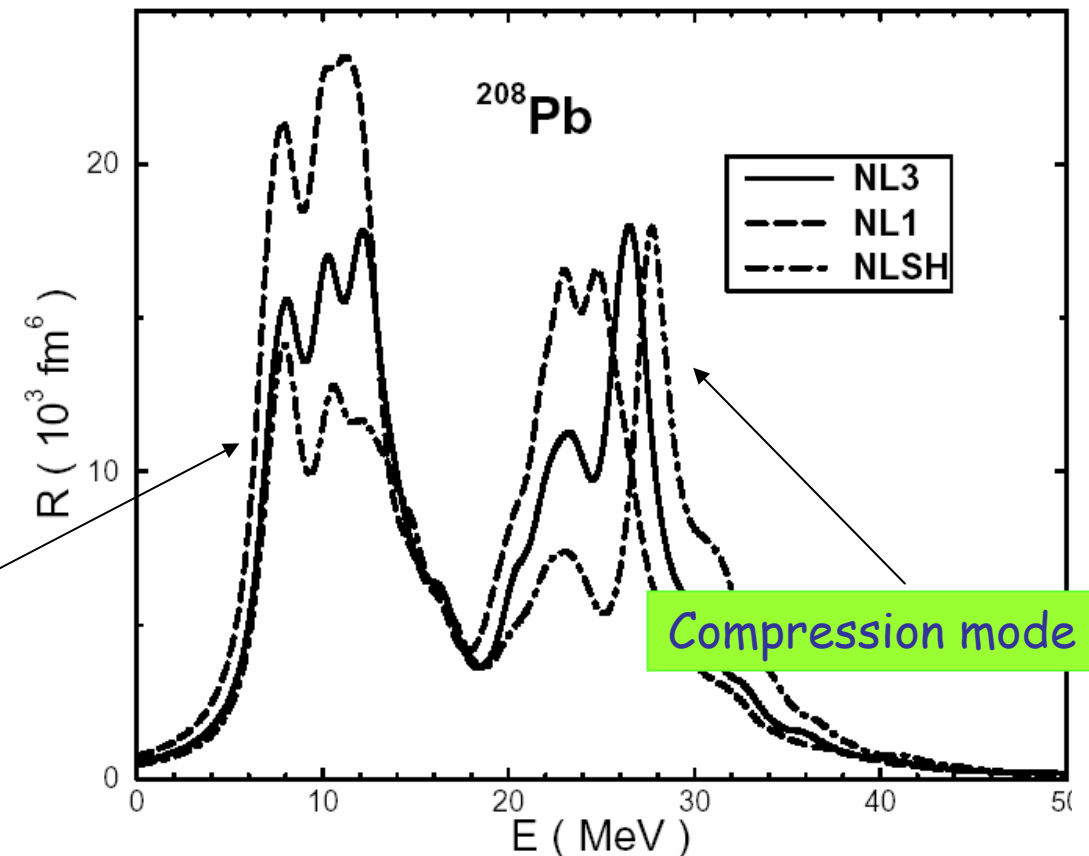
Giant isoscalar dipole oscillations \rightarrow additional information on the nuclear incompressibility.

$$\hat{Q}_{1\mu}^{T=0} = \sum_{i=1}^A \gamma_0 (r^3 - \eta r) Y_{1\mu}(\theta_i, \varphi_i)$$

ISGDR strength distributions
Effective interactions
with different K_{nm} .

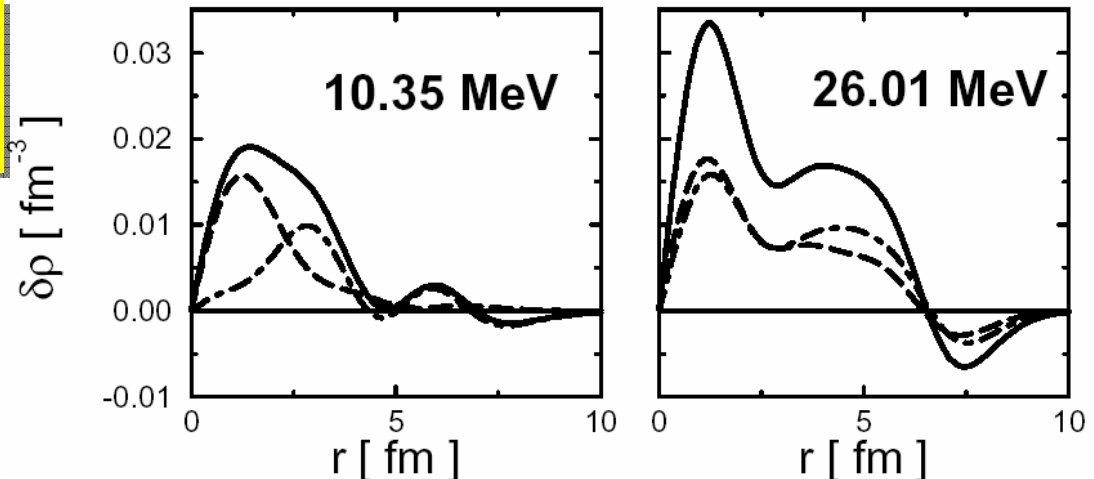
The low-energy strength
does not depend on K_{nm} !

Phys. Lett. B487, 334 (2000)



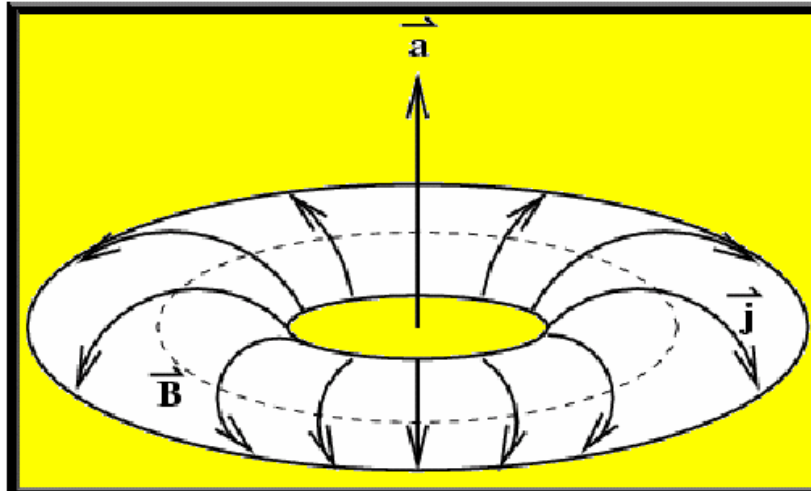
Toroidal motion:

ISGDR transition densities
for ^{208}Pb (NL3 interaction)



multipole expansion of a four-current distribution:
charge moments
magnetic moments
electric transverse moments → toroidal moments

toroidal dipole moment: poloidal currents on a torus

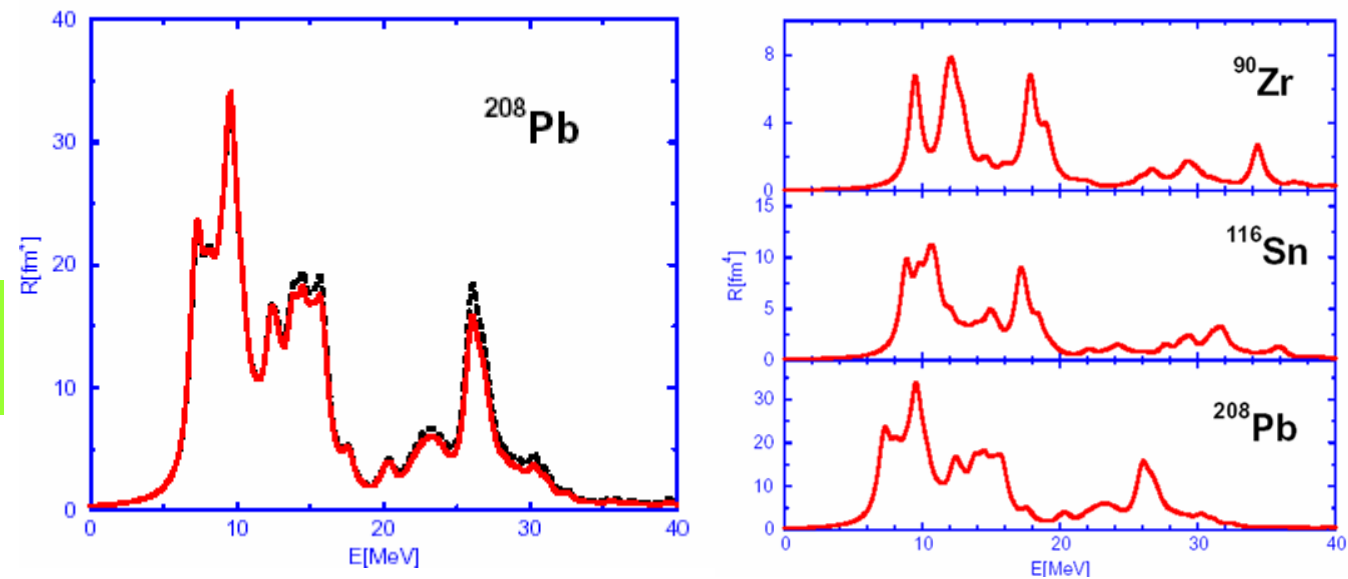


isoscalar toroidal dipole operator:

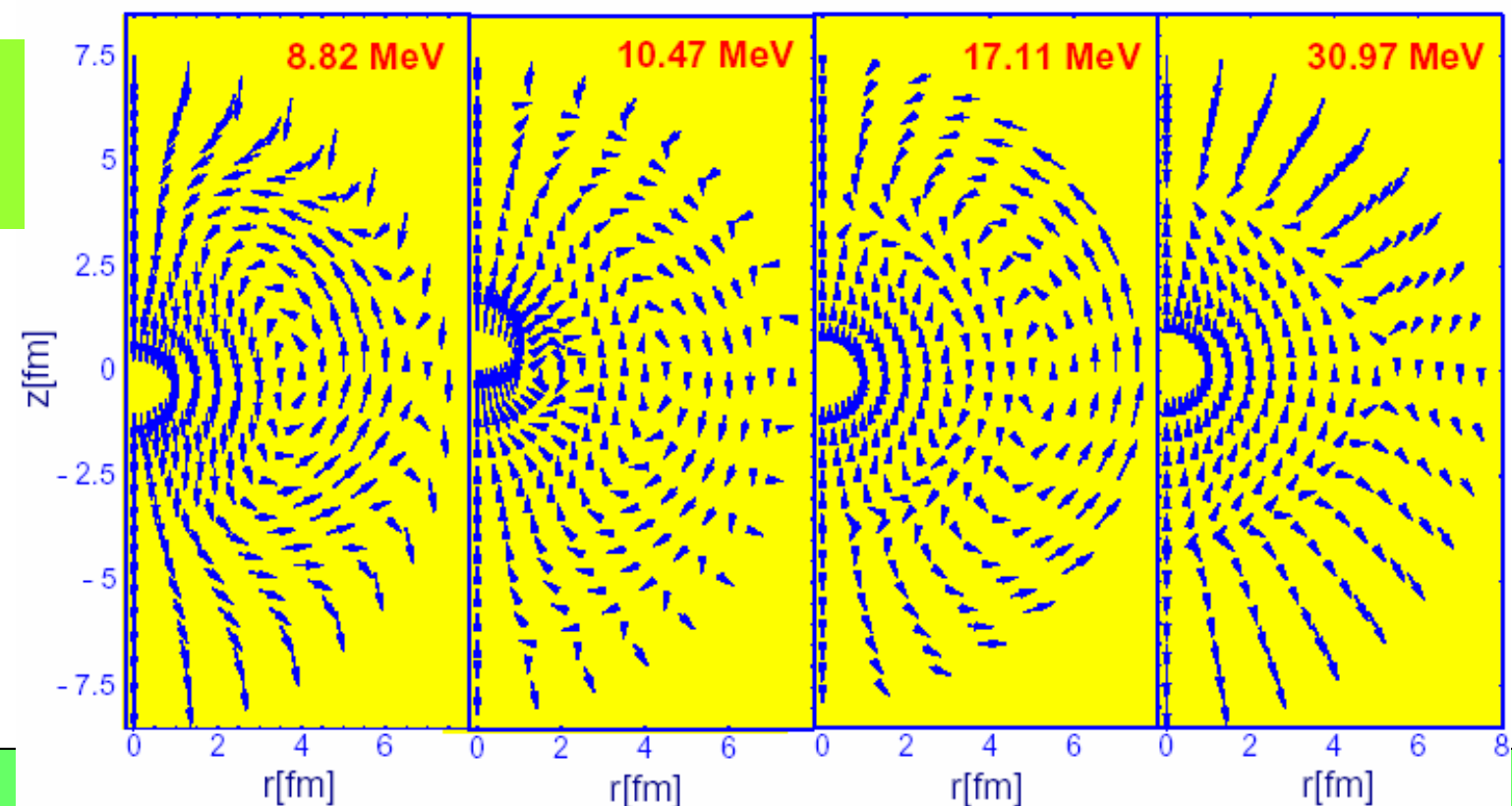
$$\hat{T}_{1\mu}^{T=0} \sim \int [r^2 \left(\vec{Y}_{10\mu}^* + \frac{\sqrt{2}}{5} \vec{Y}_{12\mu}^* \right) - \langle r^2 \rangle_0 \vec{Y}_{10\mu}^*] \cdot \vec{J}(\vec{r}) d^3r$$

Toroidal dipole
strength distributions.

Vretenar, Paar, Niksic, Ring,
Phys. Rev. C65, 021301 (2002)



Velocity
distributions
in ^{116}Sn

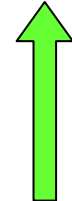


Spin-Isospin Resonances: IAR - GTR

Z, N

$Z+1, N-1$

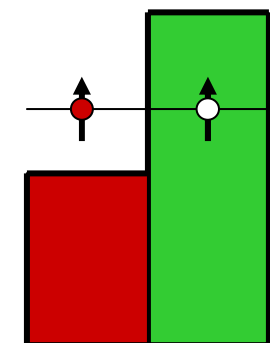
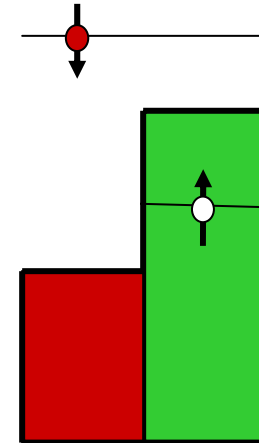
$$|GTR\rangle = S \cdot T |Z, N\rangle$$



spin flip σ

$$|Z, N\rangle \xrightarrow{\text{green arrow}} |IAR\rangle = T |Z, N\rangle$$

isospin flip τ



$$E_{GTR} - E_{IAR} \sim \Delta(l \cdot s) \sim \frac{dV}{dr} \sim \text{neutron skin} = r_n - r_p$$

Spin-Isospin Resonances: IAR and GTR

charge-exchange excitations



proton-neutron
relativistic QRPA

π and ρ -meson exchange
generate the spin-isospin
dependent interaction terms

$$\mathcal{L}_{\pi N} = -\frac{f_\pi}{m_\pi} \bar{\psi} \gamma_5 \gamma_\mu \partial^\mu \vec{\pi} \vec{\tau} \psi$$

the Landau-Migdal zero-range
force in the spin-isospin channel

$$V(1, 2) = g'_0 \left(\frac{f_\pi}{m_\pi} \right)^2 \vec{\tau}_1 \cdot \vec{\tau}_2 \Sigma_1 \cdot \Sigma_2 \delta(\mathbf{r}_1 - \mathbf{r}_2)$$

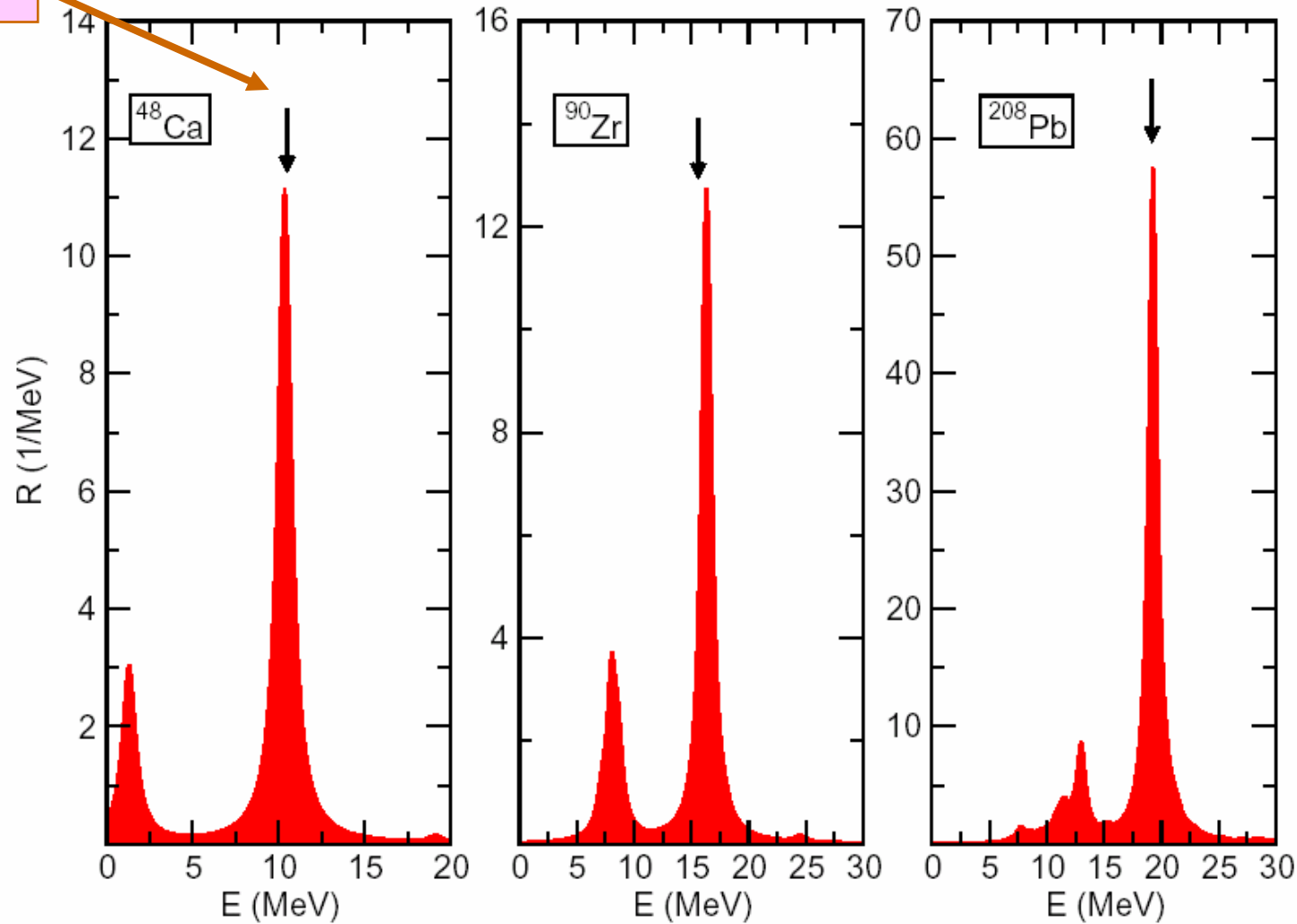
GAMOW-TELLER RESONANCE: $S=1 \ T=1 \ J^\pi = 1^+$ $(g'_0 = 0.55)$

ISOBARIC ANALOG STATE: $S=0 \ T=1 \ J^\pi = 0^+$

GT-Resonances

experiment

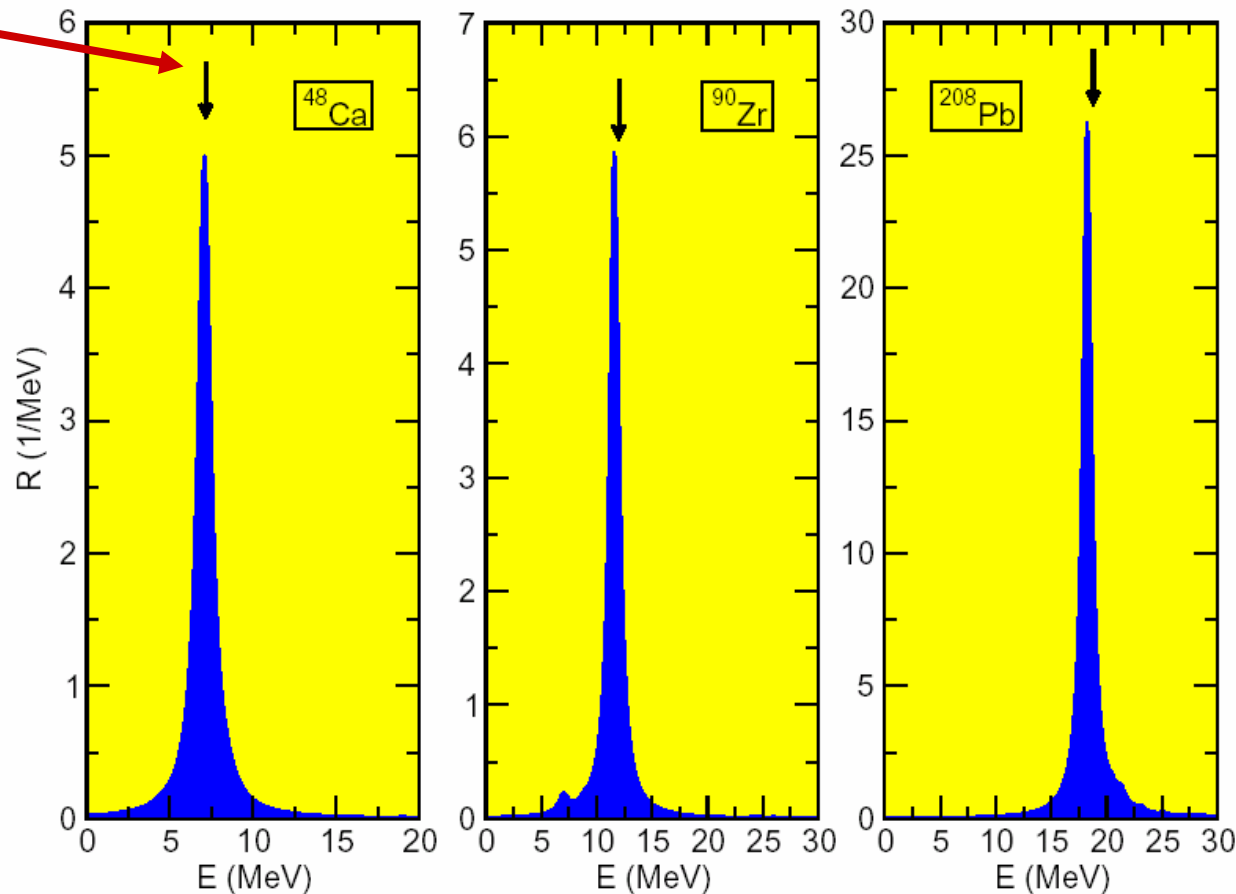
N. Paar, T. Niksic, D. Vretenar, P. Ring, PR C69, 054303 (2004)



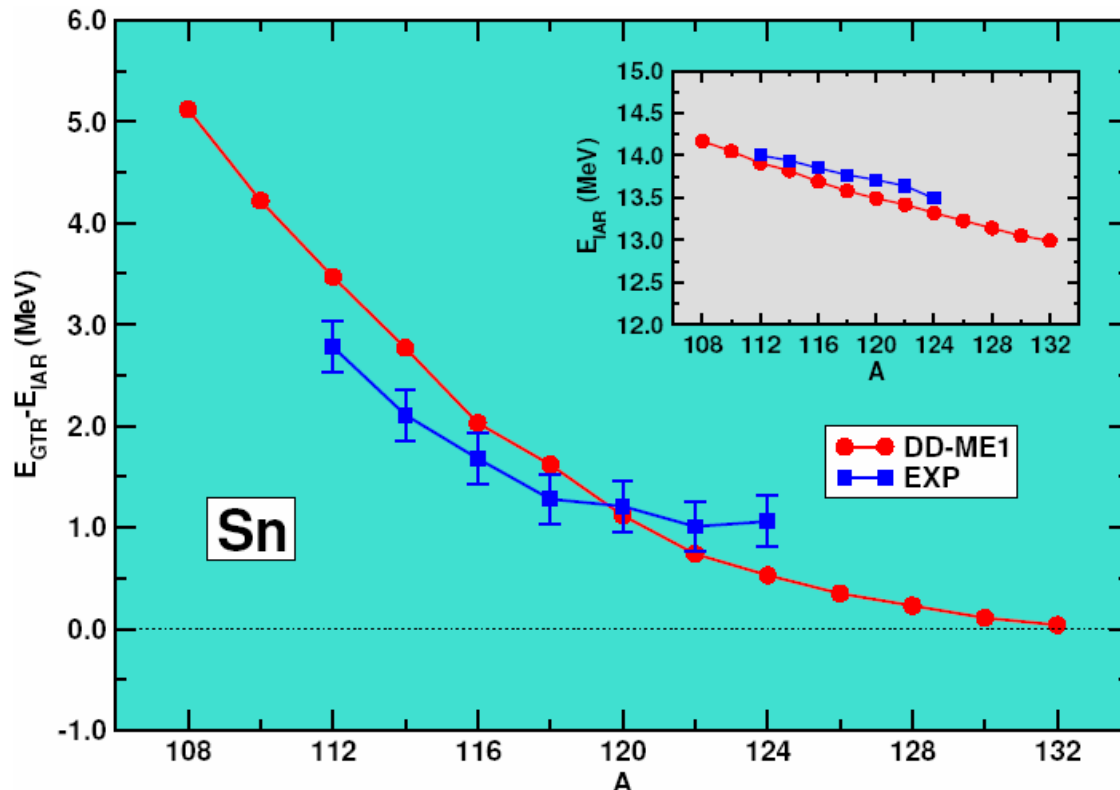
Isobaric Analog Resonance: IAR

N. Paar, T. Niksic, D. Vretenar, P. Ring, PR C69, 054303 (2004)

experiment



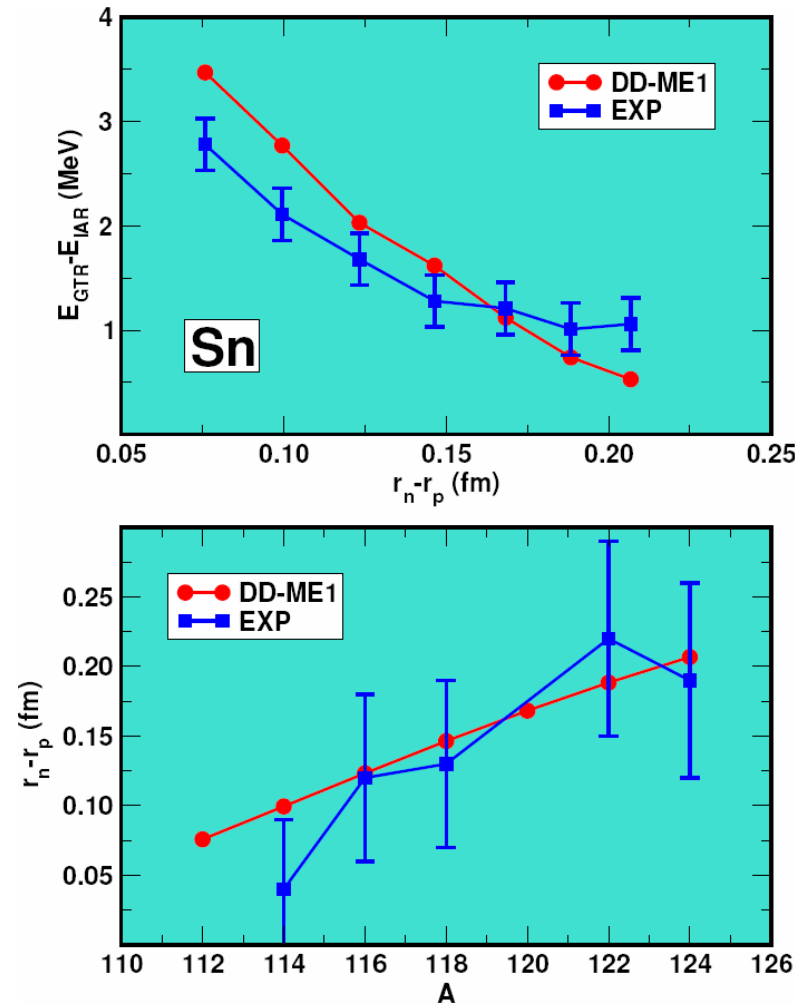
Neutron skin and IAR/GRT



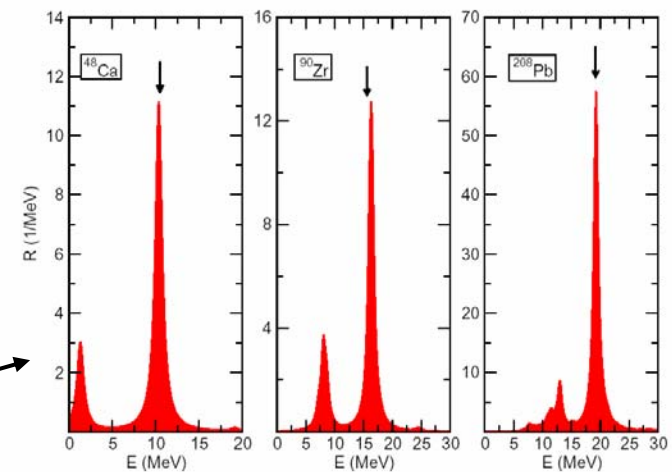
The isotopic dependence of the energy spacings between the GTR and IAS



direct information on the evolution of the neutron skin along the Sn isotopic chain



allowed β -decay :



* Important points:

- the tail of the GT-strength distribution at low energies
- the position of specific single particle levels (i.e. effective mass)
- effective pairing force in the $T=1$ and $T=0$ channel.
- in simple QRPA the lifetimes are too big

* Possible methods to improve the results:

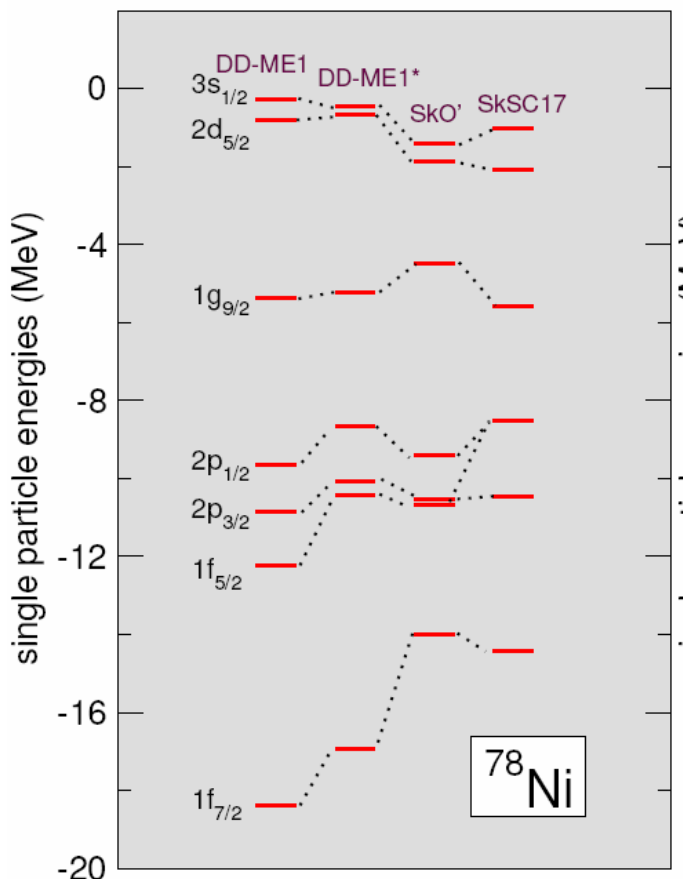
- coupling to surface vibrations (difficult and beyond mean field)
- use of a tensor coupling in the ω -channel (one phenom. param.)
- $T=0$ pairing force with Gaussian character (one phen. parameter)

enhanced value of the effective mass

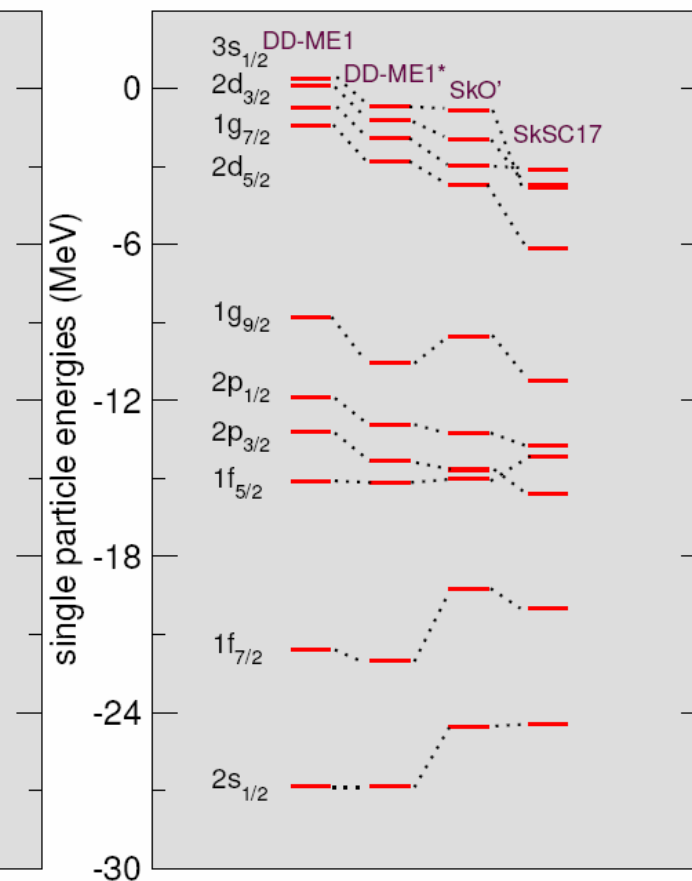


increased density of states around the Fermi surface

neutron levels



proton levels



T. Niksic et al, PRC 71, 014308 (2005)

The nucleon effective mass m^* :

m^* represents a measure of the **density of states** around the Fermi surface

nonrelativistic mean-field
models

effective mass: $m^*/m = 0.8 \pm 0.1$

relativistic mean-field
models

Dirac mass: $m_D = m + S(r)$

effective mass: $m^* = m - V(r)$

conventional
RMF models

spin-orbit splittings + nuclear matter binding



$$0.55m \leq m_D \leq 0.60m$$

$$0.64m \leq m^* \leq 0.67m$$

small density of states
-> overestimated β -decay
lifetimes

Reduction of the spin-orbit in neutron-rich nuclei

Lalazissis, Vretenar, Poeschl, Ring, Phys. Lett. B418, 7 (1998)

The spin-orbit potential originates from the addition of two large fields: the field of the vector mesons (short range repulsion), and the scalar field of the sigma meson (intermediate attraction).

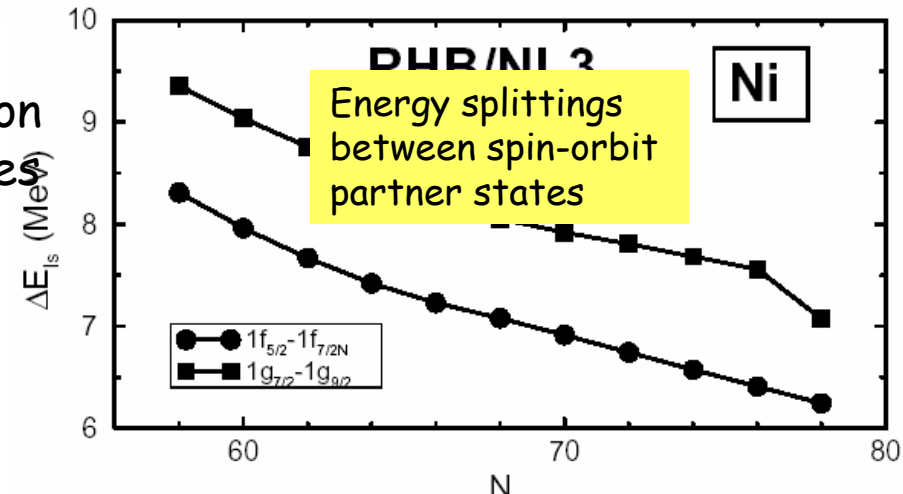
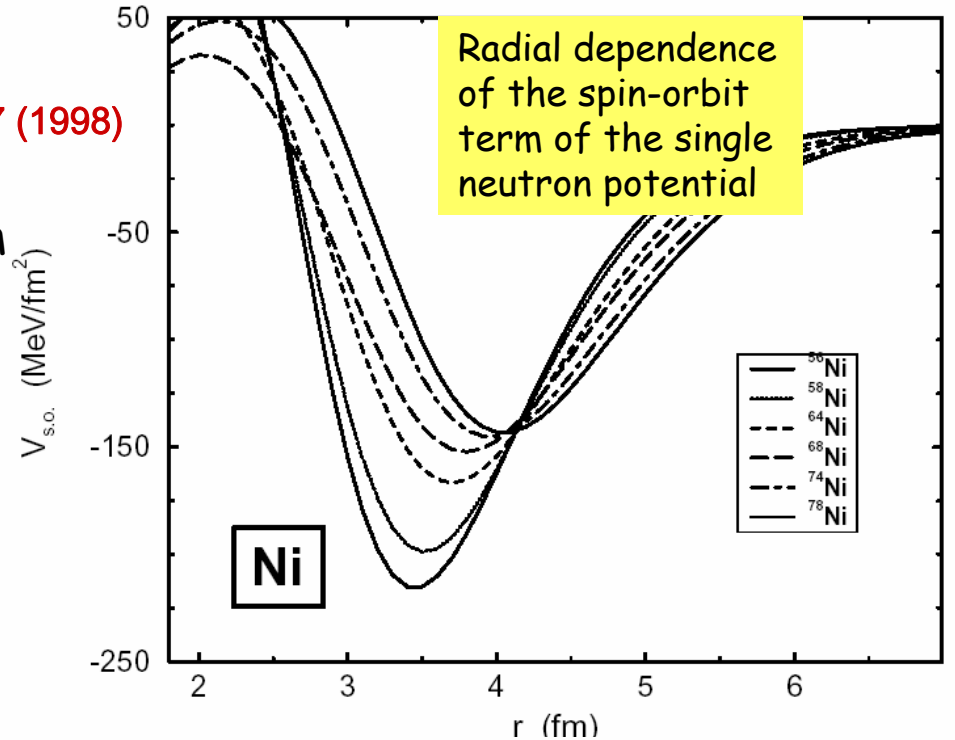
$$V_{s.o.} \approx \frac{1}{r} \frac{\partial}{\partial r} V_{ls}(r)$$

$$V_{ls} = \frac{m}{m_{eff}}(V - S)$$

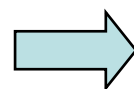
weakening of the effective single-neutron spin-orbit potential in neutron-rich isotopes

→ reduced energy spacings between spin-orbit partners

$$\Delta E_{ls} = E_{n,l,j=l-1/2} - E_{n,l,j=l+1/2}$$

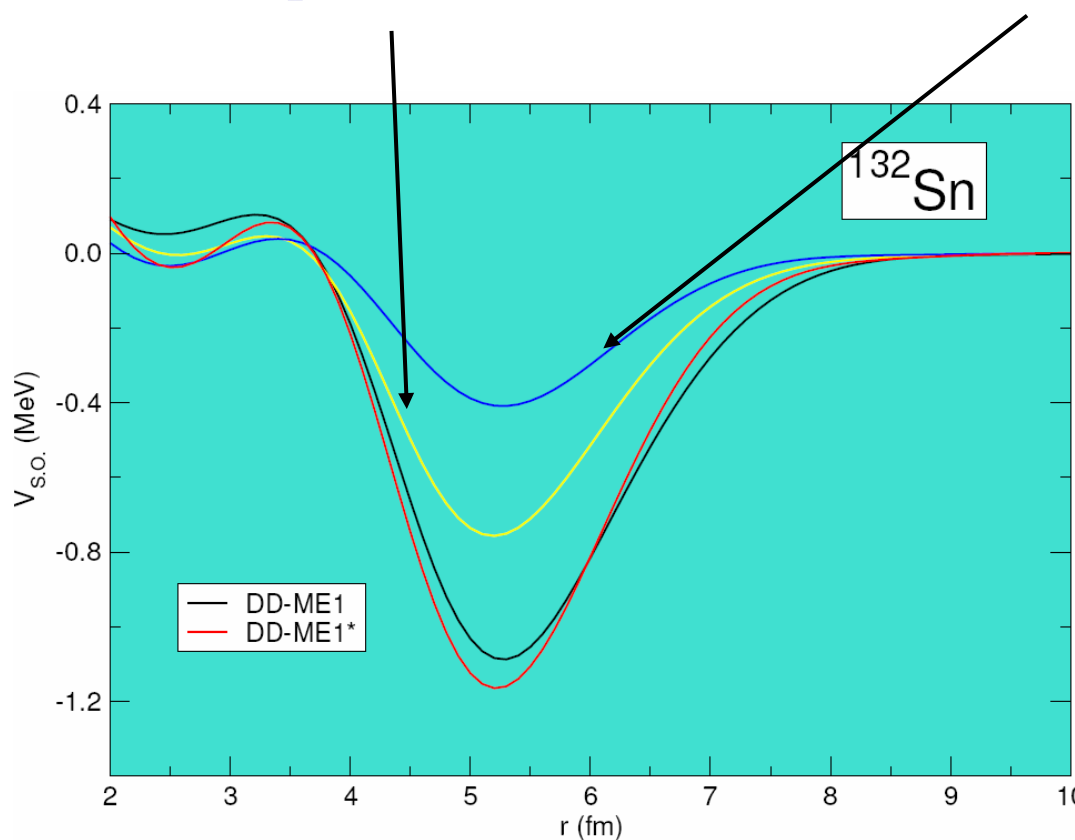


tensor omega-nucleon coupling
enhances the spin-orbit interaction



scalar and vector self-energies
can be reduced

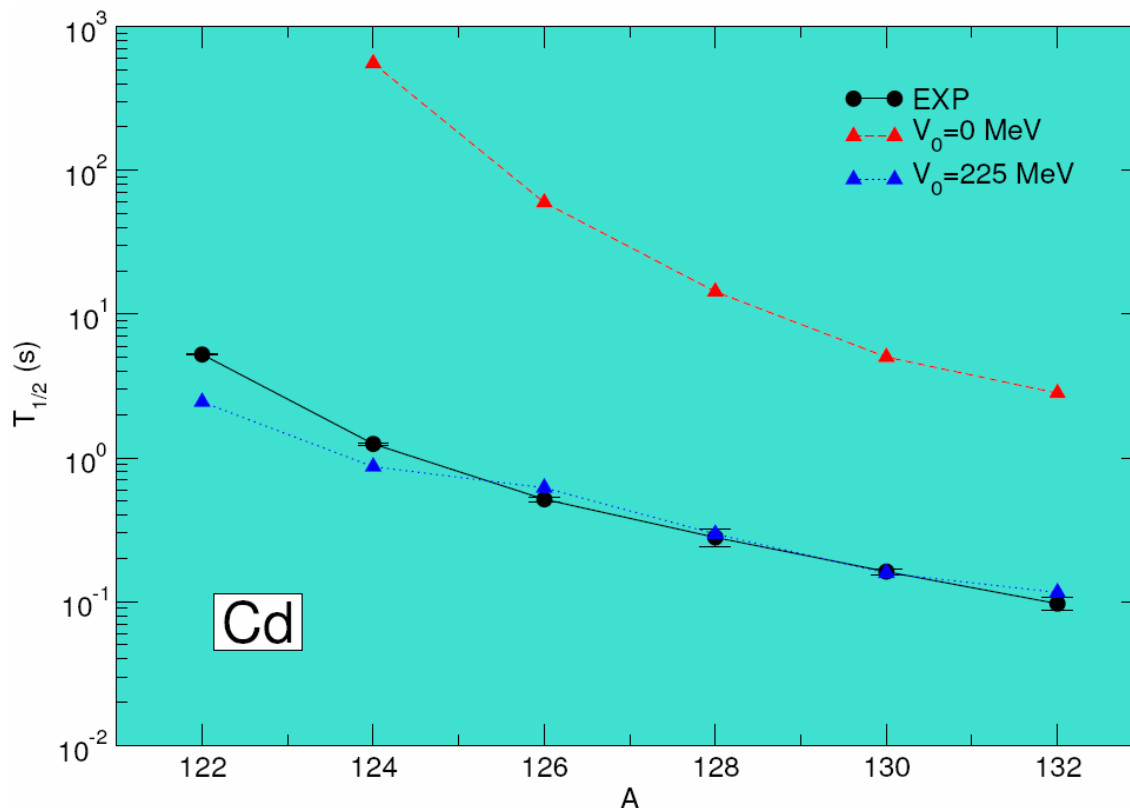
$$V_{SO} = \left[\frac{1}{4\bar{M}^2} \frac{1}{r} \frac{d}{dr} (V - S) + \frac{f_V}{2M\bar{M}} \frac{1}{r} \frac{d\omega}{dr} \right] \mathbf{l} \cdot \mathbf{s}$$



T. Niksic et al., PRC 71, 014308 (2005)

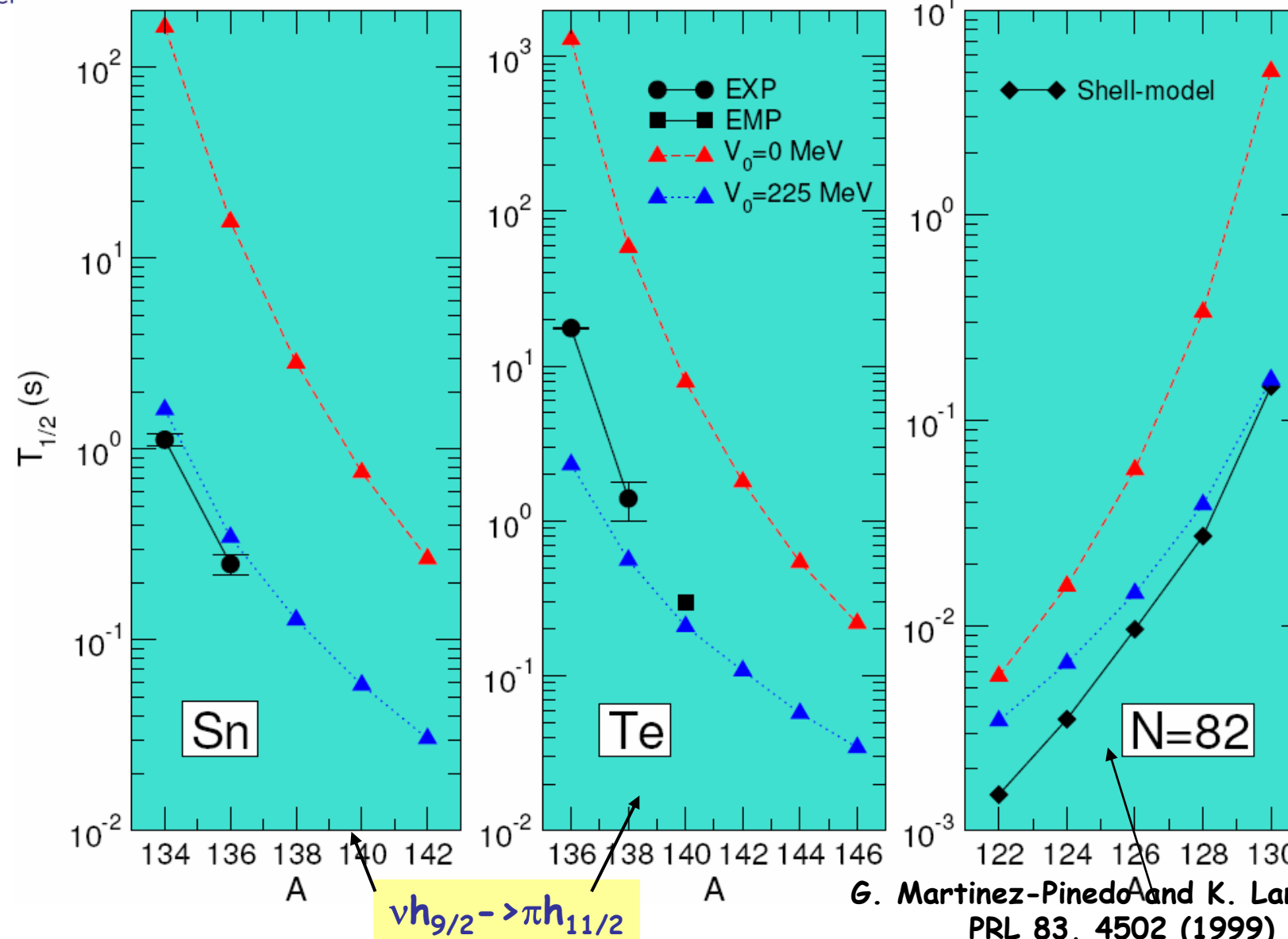
N≈82 region:

Cadmium isotopes: $\pi 1g9/2$ level is partially empty
 → T=0 pairing has large influence on the $v1g7/2 \rightarrow \pi 1g9/2$ transition
 which dominates the β -decay process



T. Niksic et al, PRC 71, 014308 (2005)

An **increase** of the T=0 pairing **partially compensates** for the fact
that the density of states is still rather low Niksic et al, PRC 71, 014308 ('05)



Correlations beyond mean field

- Conservation of symmetries by projection before variation
- Motion with large amplitude by Generator Coordinates
- Coupling to collective vibrations
 - shifts of single particle energies
 - decay width of giant resonances

Projected Density Functionals

$$|\Psi^N\rangle = \hat{P}^N |\Phi\rangle = \delta(\hat{N} - N) |\Phi\rangle = \int \frac{d\varphi}{2\pi} e^{i\varphi(\hat{N} - N)} |\Phi\rangle$$

projected density functional:

$$E^N[\hat{\rho}, \hat{\kappa}] = \frac{\langle \Phi | \hat{H} \hat{P}^N | \Phi \rangle}{\langle \Phi | \hat{P}^N | \Phi \rangle}$$

analytic expressions

projected HFB-equations (variation after projection):

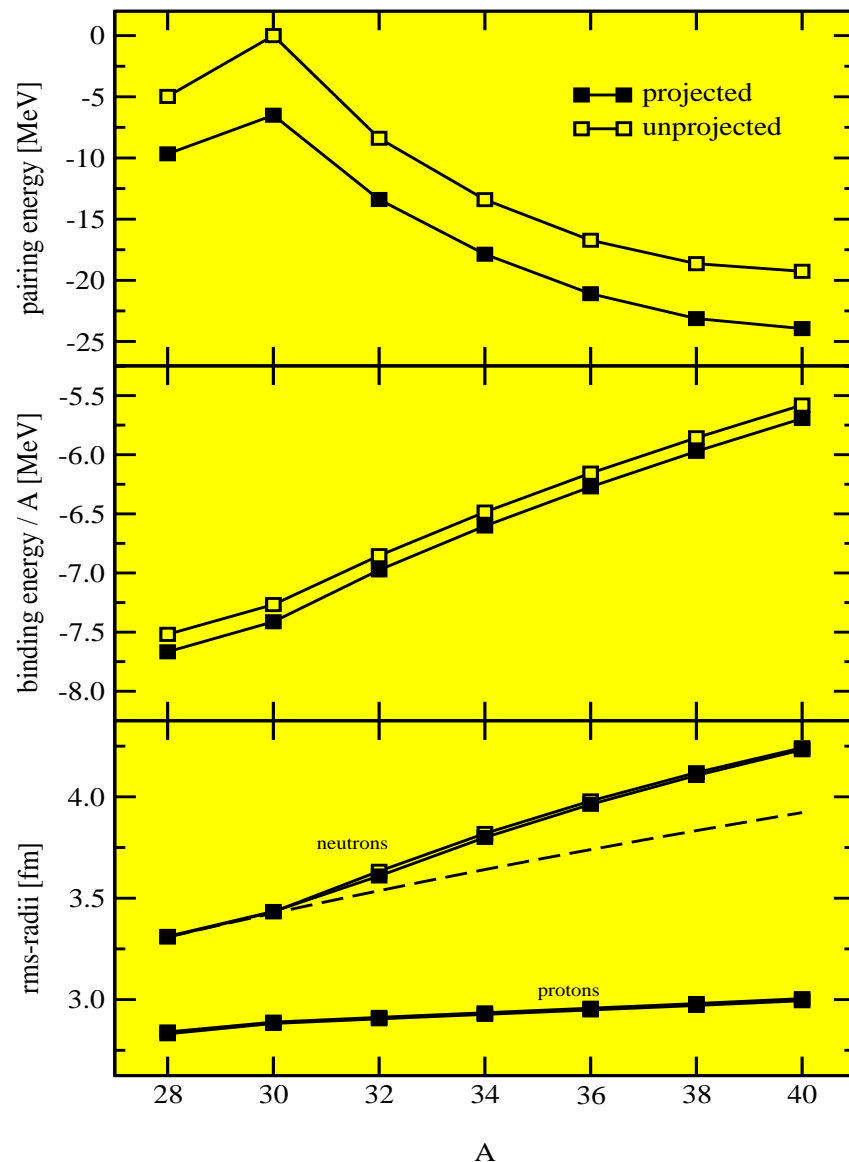
$$\begin{pmatrix} \hat{h}^N & \hat{\Delta}^N \\ -\Delta^{N*} & -\hat{h}^{N*} \end{pmatrix} \begin{pmatrix} U_k(\mathbf{r}) \\ V_k(\mathbf{r}) \end{pmatrix} = \begin{pmatrix} U_k(\mathbf{r}) \\ V_k(\mathbf{r}) \end{pmatrix} E_k$$

J.Sheikh and P. Ring NPA 665 (2000) 71

$$\hat{h}^N = \frac{\delta E^N}{\delta \hat{\rho}}$$

$$\hat{\Delta}^N = \frac{\delta E^N}{\delta \hat{\kappa}}$$

Ne-isotopes



pairing energies

binding energies

rms-radii

L. Lopes, PhD Thesis, TUM, 2002

Generator Coordinate Method (GCM)

$$\langle \delta\Phi | \hat{H} - q\hat{Q} | \Phi \rangle = 0$$

Constraint Hartree Fock produces wave functions depending on a generator coordinate q

$$|q\rangle = |\Phi(q)\rangle$$

GCM wave function is a superposition of Slater determinants

$$|\Psi\rangle = \int dq f(q) |q\rangle$$

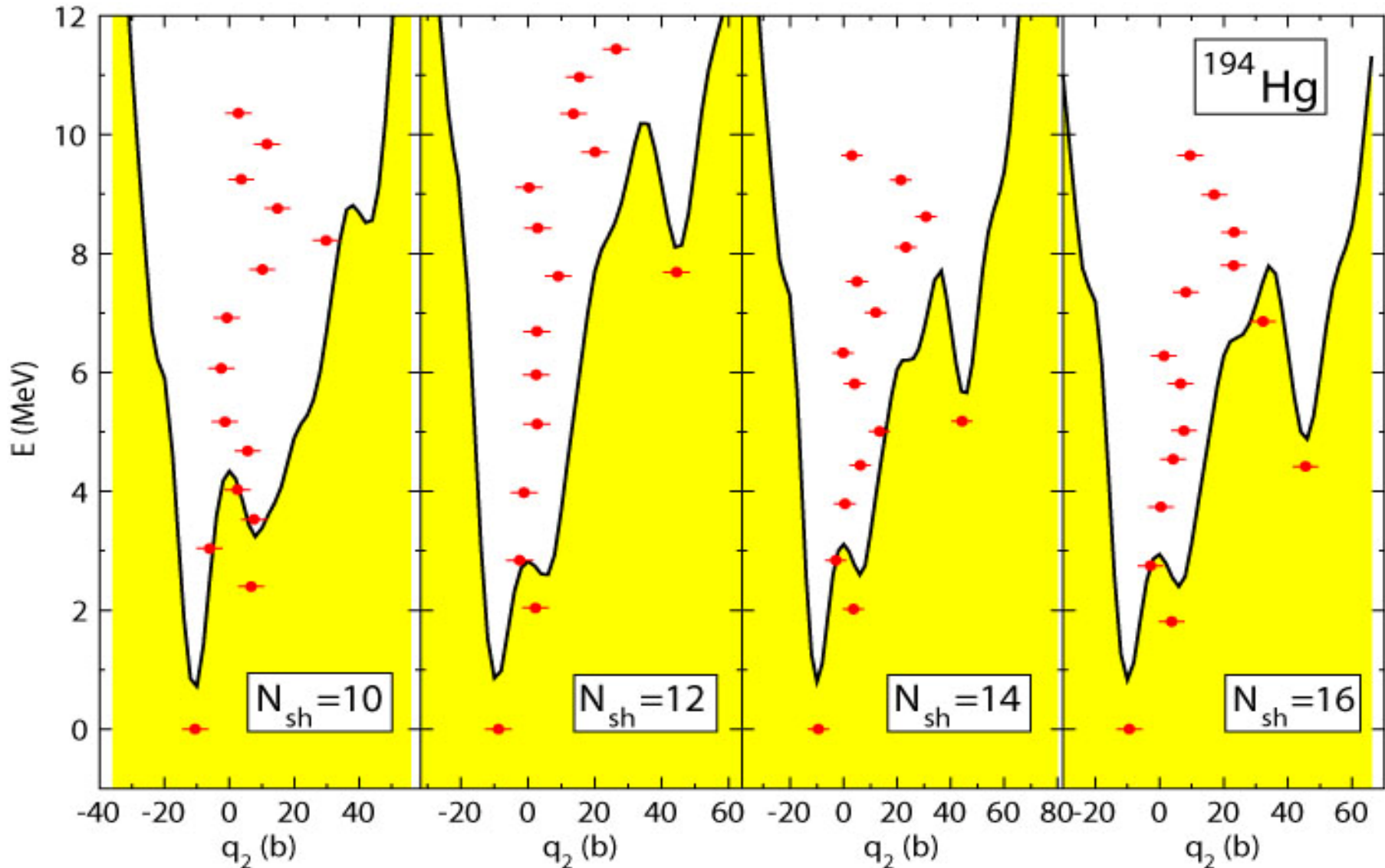
Hill-Wheeler equation:

$$\int dq \left[\langle q | H | q' \rangle - E \langle q | q' \rangle \right] f(q') = 0$$

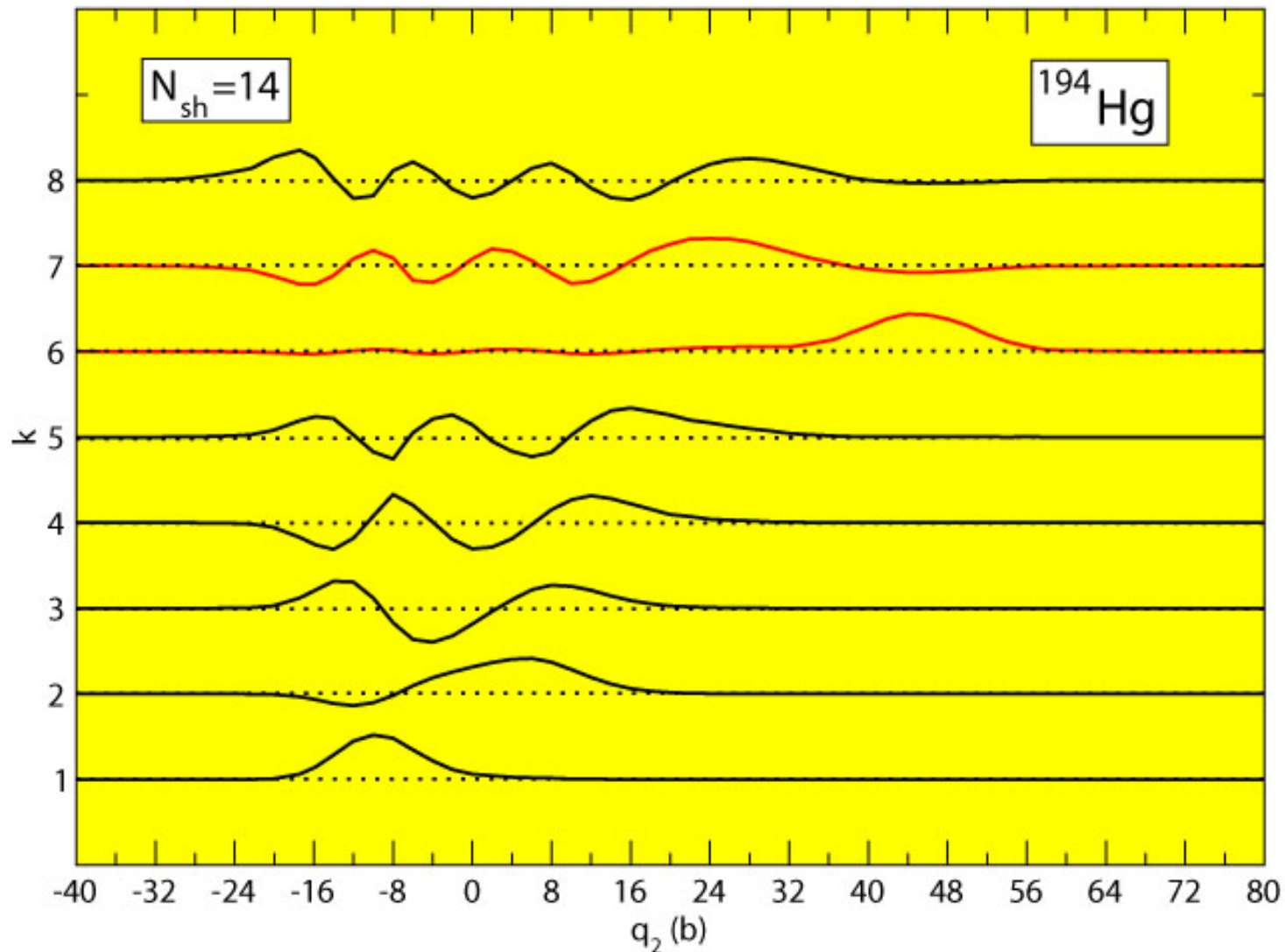
with projection:

$$|\Psi\rangle = \int dq f(q) \hat{P}^N \hat{P}^I |q\rangle$$

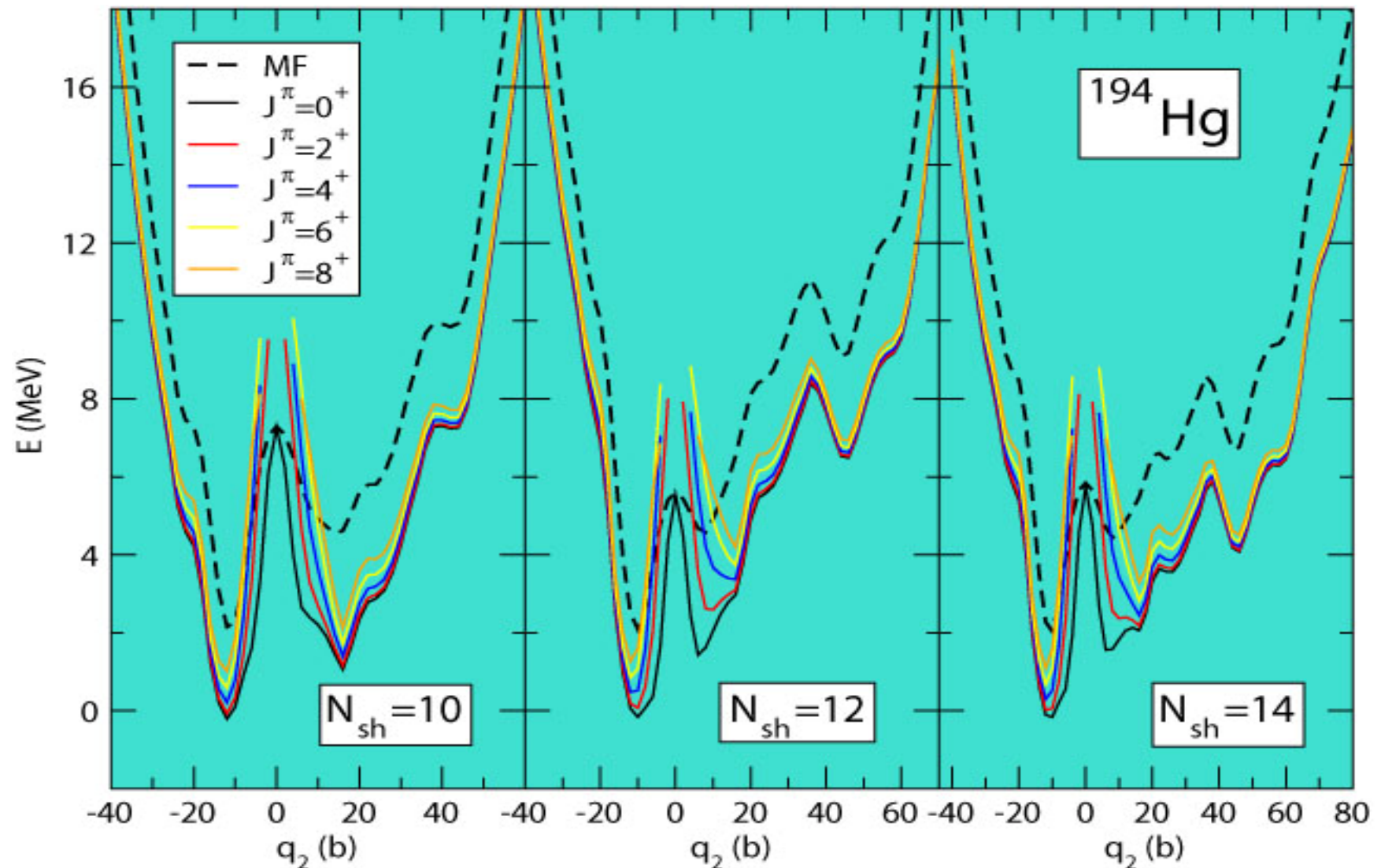
GCM without projection:



GCM-wave functions of the lowest states



Ang. momentum projected energy surfaces:



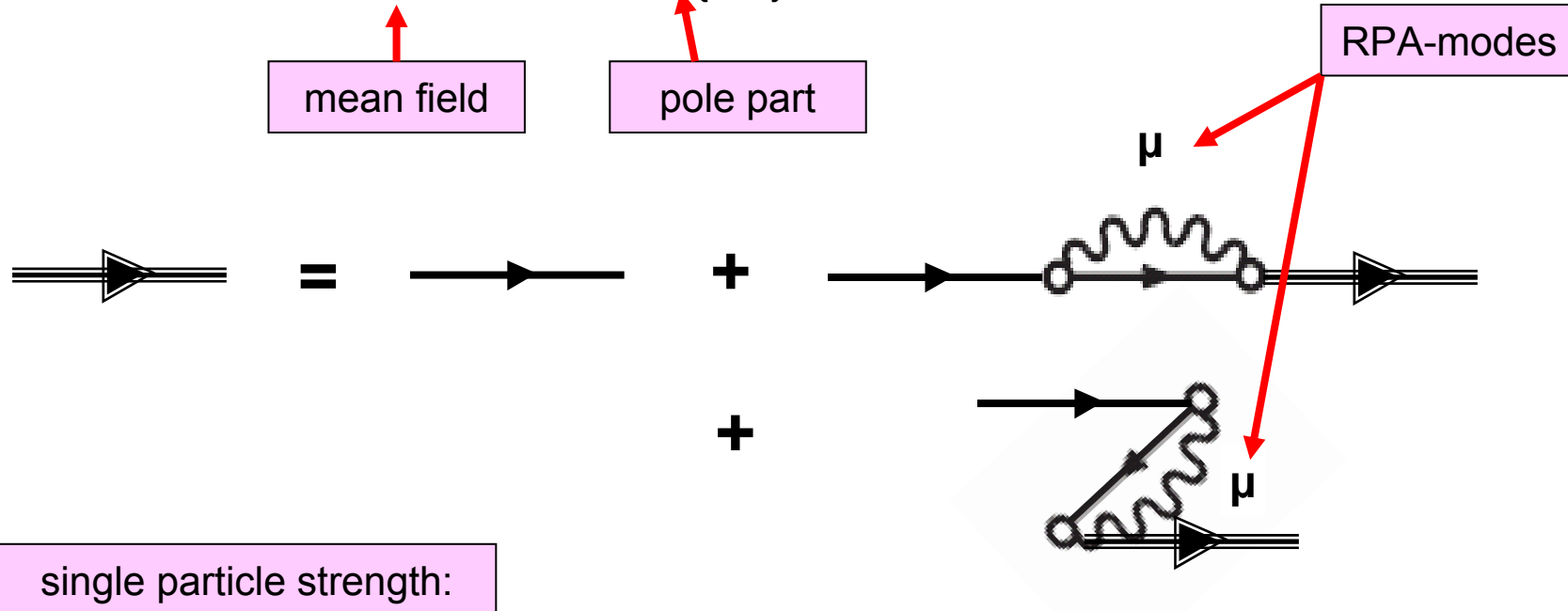
Vibrational Couplings: energy dependent self-energy:

$$\Sigma = S + V + \Sigma(\omega)$$

mean field

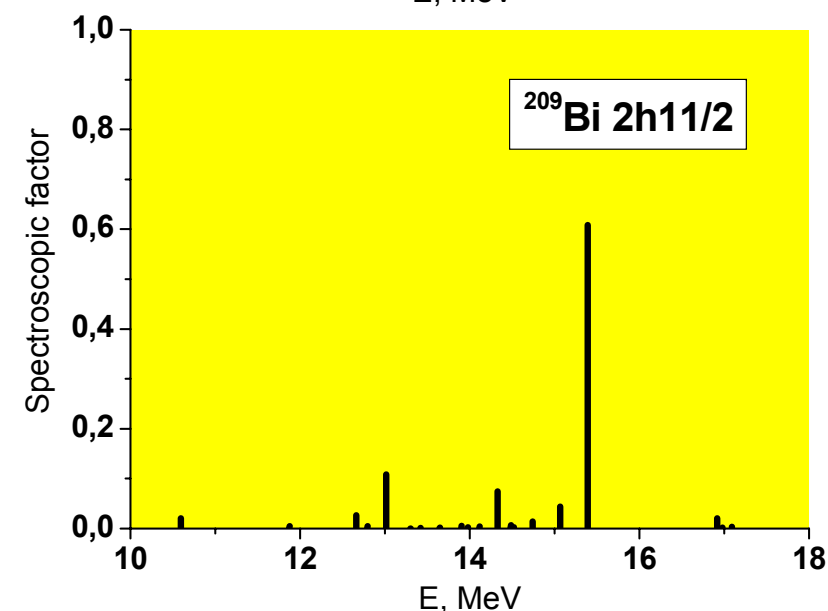
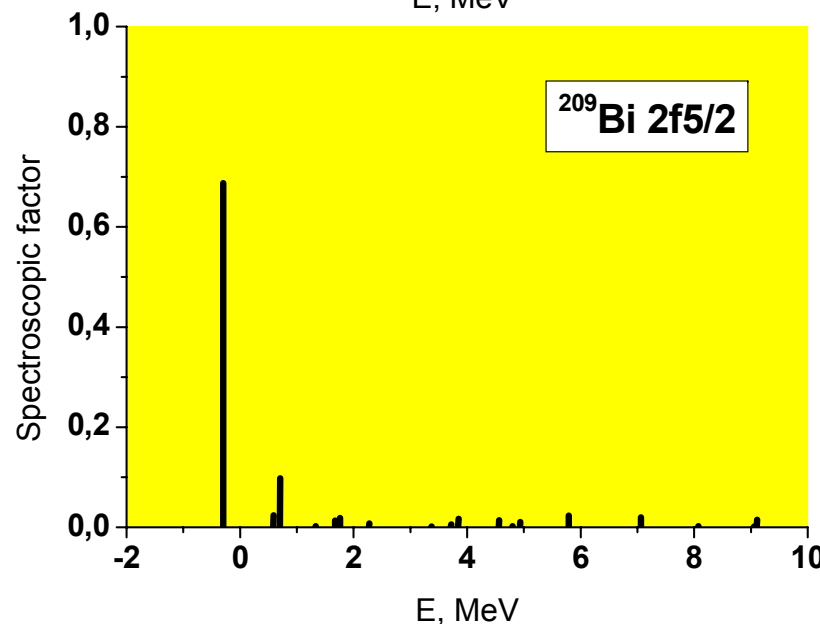
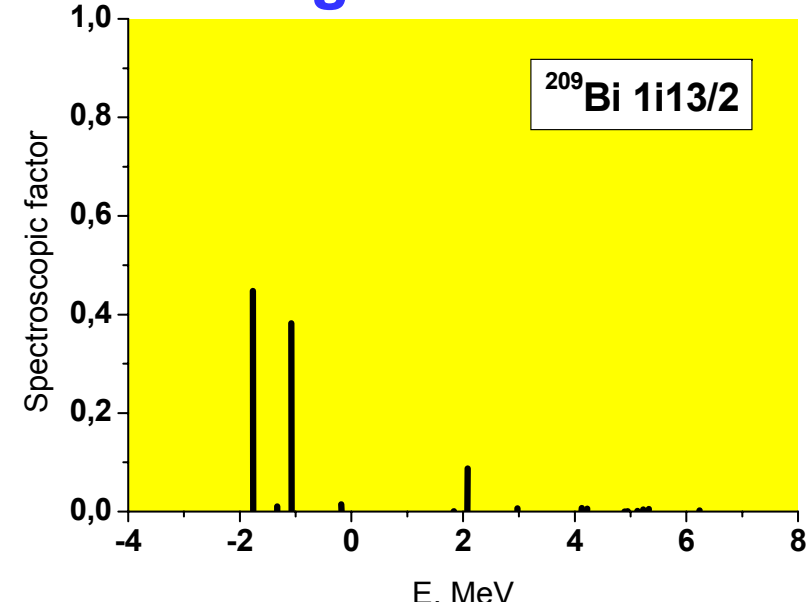
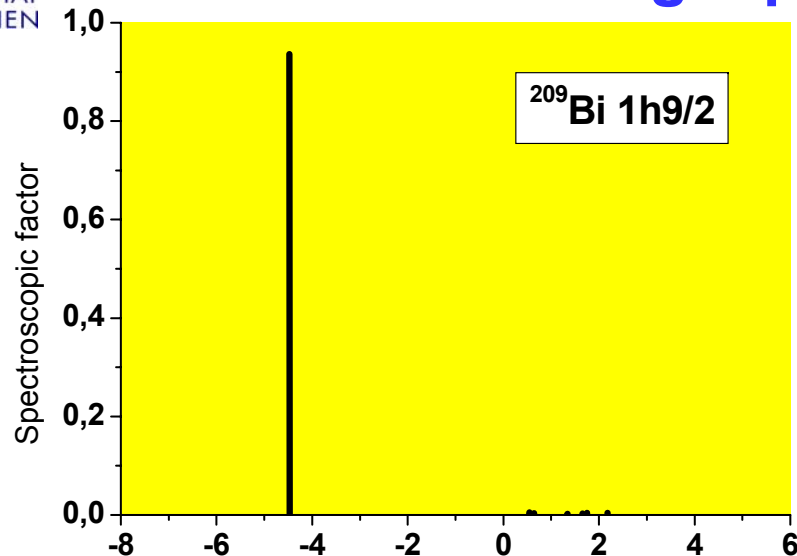
pole part

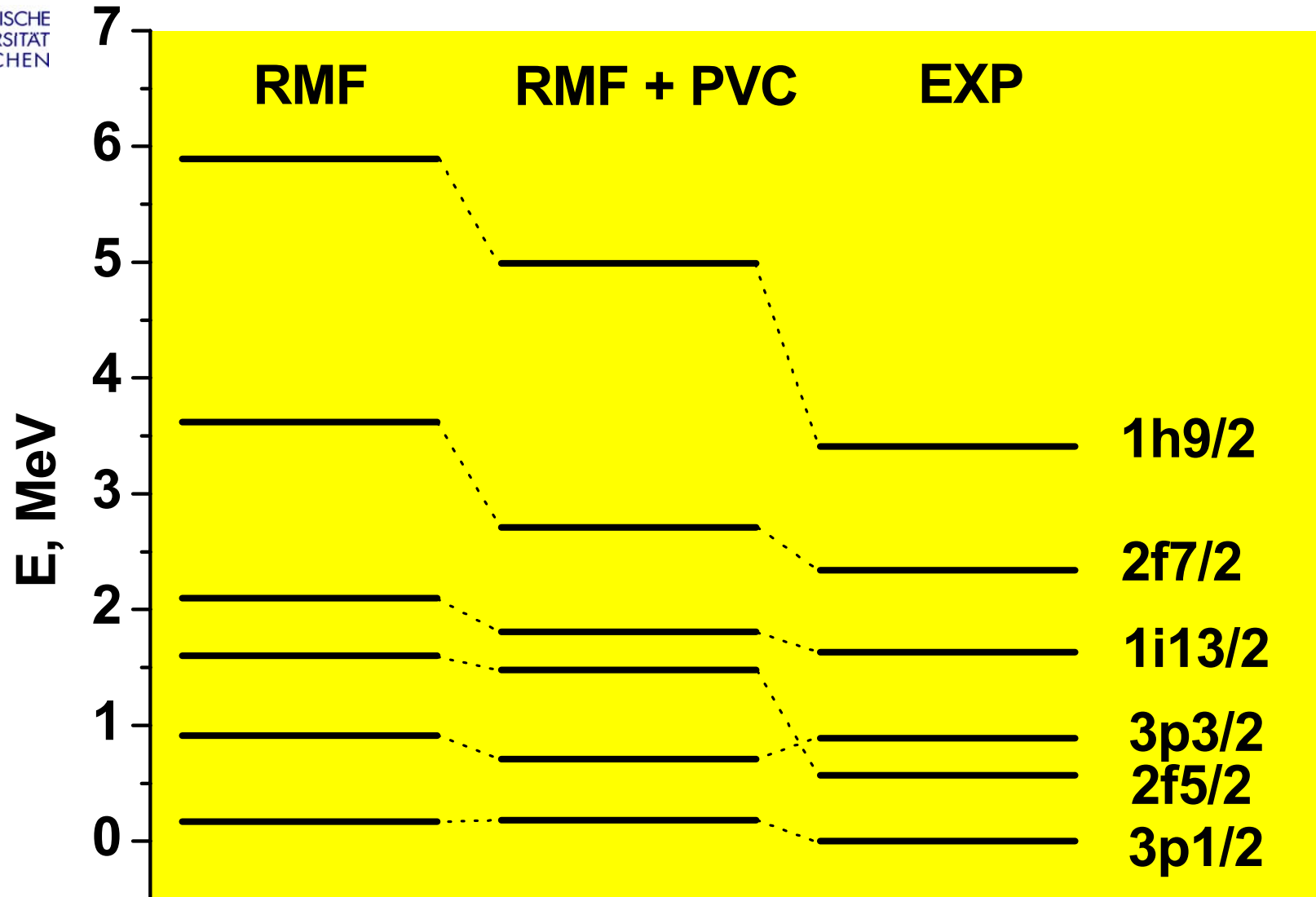
RPA-modes



$$z_\nu = \left[1 - \frac{d\Sigma_{\nu\nu}}{d\omega} \Big|_{\omega=\epsilon_\nu} \right]^{-1}$$

Distribution of single-particle strength in ^{209}Bi

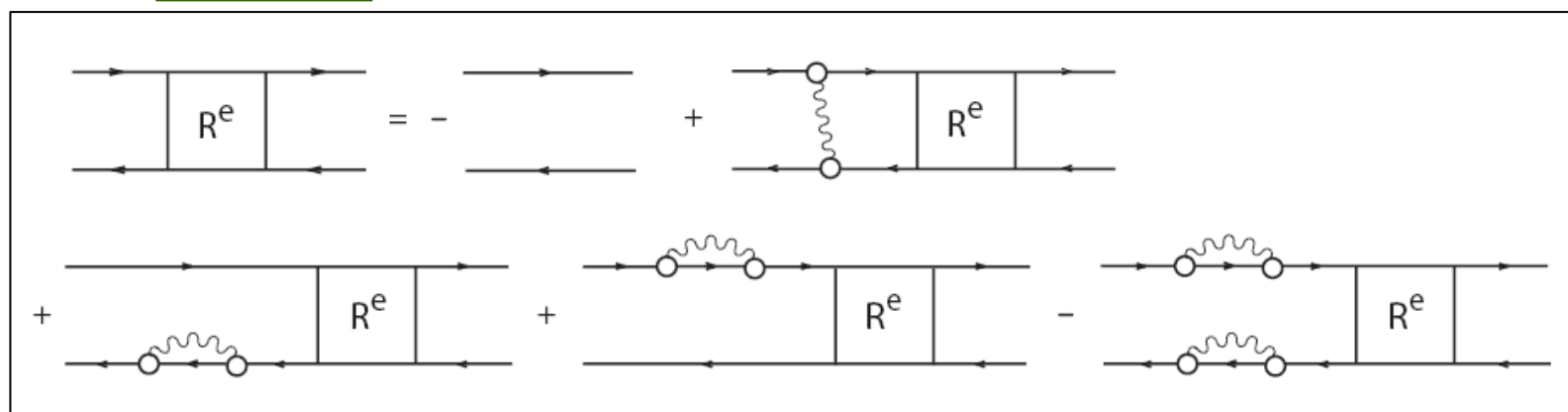
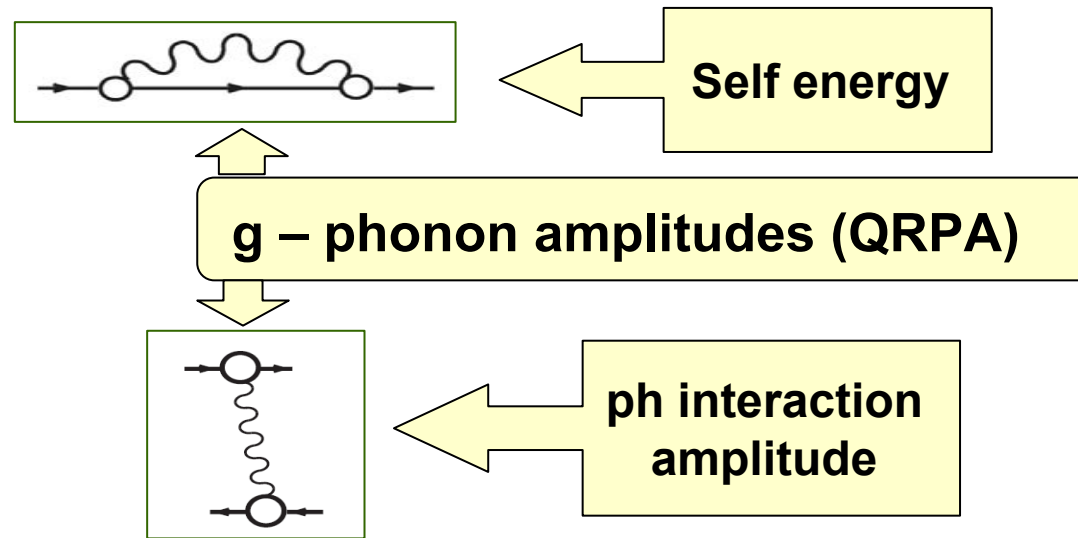




Level scheme for ^{207}Pb

Contributions of complex configurations

The full response contains energy dependent parts coming from vibrational couplings.

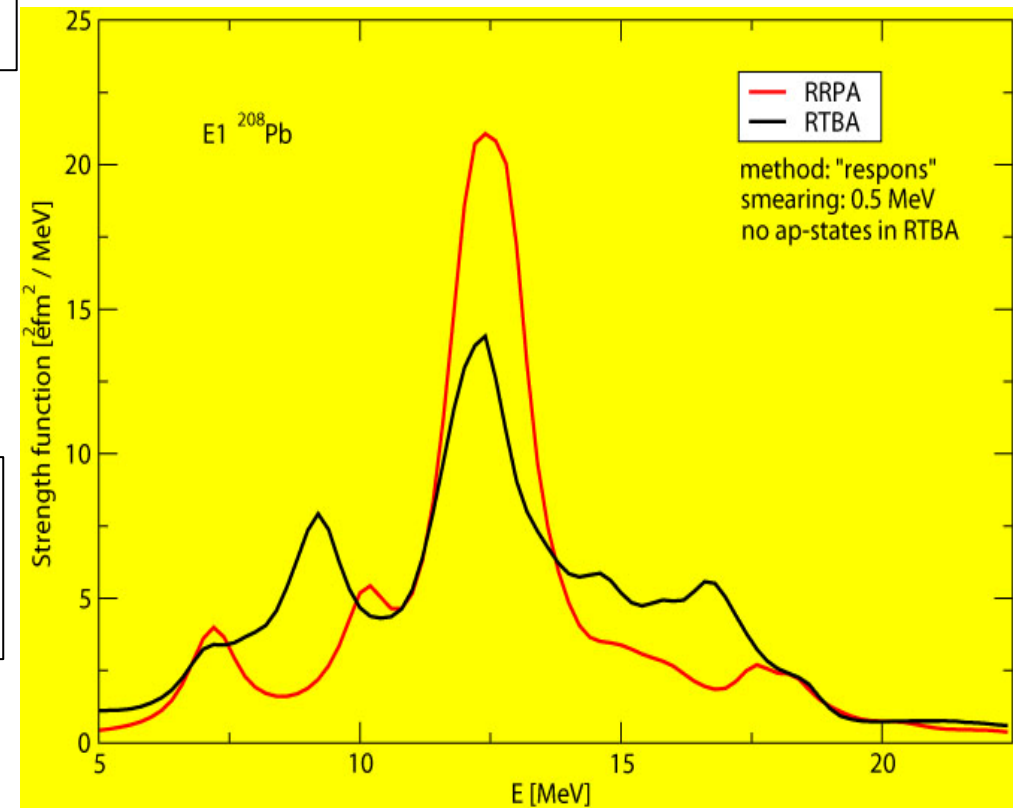


Decay-width of the Giant Resonances

$$S(E) = -\frac{1}{\pi} \operatorname{Im} \Pi(E + i \Delta)$$

E1 photoabsorption cross section

$$\sigma_{E1}(E) = \frac{16\pi^3 e^2}{9\hbar c} E S_{E1}(E)$$



Conclusions

**On the way to a universal covariant density functional
adjusted to ground state properties of finite nuclei.
≈7 parameters necessary for high precision**

**Time-dependent mean field theory provides a
parameter-free theory for excited states**

- **rotational spectra (cranked RHB-theory)**
- **vibrational excitations (rel. QRPA)**

Method beyond mean field:

- **Projected functionals (PDFT)**
- **Generator Coordinate Method (GCM)**
- **Particle-Vibrational Coupling (PVC)**

Open Problems:

Fock terms and tensor forces:

- why is the first order pion-exchange quenched?

Vacuum polarization:

- renormalization in finite systems

Simpler parametrizations:

- point coupling
- simple pairing

Do we have to change the functional,
if we go beyond mean field?

Open Problems:

Fock terms and tensor forces:

- why is the first order pion-exchange quenched?

Vacuum polarization:

- renormalization in finite systems

Simpler parametrizations:

- point coupling
- simple pairing

Do we have to change the functional,
if we go beyond mean field?

Colaborators:

A. V. Afanasjev (Mississippi)

G. A. Lalazissis (Thessaloniki)

D. Vretenar (Zagreb)

E. Litvinova (Obninsk)

T. Niksic (Zagreb)

N. Paar (TU Darmstadt)

E. Lopes (BMW)

D. Pena (TU Munich)

A. Wandelt (Telekom)